energies

MDPI

Article

A Decoupling Rolling Multi-Period Power and Voltage Optimization Strategy in Active Distribution Networks

Xiaohui Ge [1], Lu Shen [2,*], Chaoming Zheng [3], Peng Li [1] and Xiaobo Dou [2]

[1] Electric Power Research Institute of State Grid Zhejiang Electric Power Company, Hangzhou 310014, China; gegexiaohui@126.com (X.G.); lipeng_hz@163.com (P.L.)
[2] Department of Electrical Engineering, Southeast University, Nanjing 210096, China; xiaobodou@seu.edu.cn
[3] State Grid Zhejiang Electric Power Corporation, Hangzhou 310007, China; 13588124939@139.com
* Correspondence: 230179583@seu.edu.cn

Received: 7 September 2020; Accepted: 1 November 2020; Published: 5 November 2020

Abstract: With the increasing penetration of distributed photovoltaics (PVs) in active distribution networks (ADNs), the risk of voltage violations caused by PV uncertainties is significantly exacerbated. Since the conventional voltage regulation strategy is limited by its discrete devices and delay, ADN operators allow PVs to participate in voltage optimization by controlling their power outputs and cooperating with traditional regulation devices. This paper proposes a decoupling rolling multi-period reactive power and voltage optimization strategy considering the strong time coupling between different devices. The mixed-integer voltage optimization model is first decomposed into a long-period master problem for on-load tap changer (OLTC) and multiple short-period subproblems for PV power by Benders decomposition algorithm. Then, based on the high-precision PV and load forecasts, the model predictive control (MPC) method is utilized to modify the independent subproblems into a series of subproblems that roll with the time window, achieving a smooth transition from the current state to the ideal state. The estimated voltage variation in the prediction horizon of MPC is calculated by a simplified discrete equation for OLTC tap and a linearized sensitivity matrix between power and voltage for fast computation. The feasibility of the proposed optimization strategy is demonstrated by performing simulations on a distribution test system.

Keywords: active distribution network; reactive power and voltage optimization; decoupled multiple periods; benders decomposition; model predictive control

1. Introduction

The rapid penetration of distributed photovoltaics (PVs) in active distribution networks (ADNs) has considerably challenged the operation mode of the traditional grid [1]. Some research indicates that one of the major constraints for promoting PV integration into ADNs is voltage stability [2,3]. The voltage at the end of feeder will rise if the intermittent production of PV generation causes power flow reversal [4,5]. Since undesirable voltage violations may cause serious negative effects [6], an appropriate effective reactive power and voltage strategy is required to solve these problems.

The on-load tap changer (OLTC) in distribution networks is considered to be a typical control device to prevent the violations of voltages, which keeps the substation secondary bus voltage constant by adjusting the tap position [7]. However, due to physical constraints and low cost benefit ratios, it cannot change flexibly to achieve real-time adjustment [8,9]. Recently, the continuous, quick and frequent reactive power outputs of distributed generation are appealing to mitigate voltage violations and fluctuations [10,11], which avoids adding extra voltage devices and reactive compensators in ADN. The authors of [12,13] presented an optimized decentralized control approach for each PV

inverter based on voltage sensitivity analysis by implementing the control action at the point of common coupling (PCC) [14] as one of ancillary services to the ADN. A multi-mode adaptive local reactive power control method based on Q(P) characteristics is discussed in [15] considering control parameter optimization. Reference [16] proposed a combination of centralized-remote control and local-decentralized control to ensure that the nodal voltages remain within regulatory limits. Although these studies have fully demonstrated that distributed PVs have the ability to enhance power quality as well as reliability of the system [17], their reactive outputs are limited by capacity and power factor. Moreover, the line equivalent impedance directly affects the voltage regulation. the R/X ratio determines the influence of the active power and reactive power injected by distributed generation on the node voltage [18]. For the low-reactance cables, it is more difficult to try to keep the voltage within the allowable range by adjusting the reactive power output of distributed generations. The fluctuation of PV active power output greatly affects the node voltage. When serious violations occur, it is insufficient to correct serious violations by distributed PVs alone, which requires cooperation with traditional adjustment devices [19]. It follows that the reactive power and voltage optimization model of ADN is a complex mixed integer nonlinear programming (MINP) problem, not only dealing with continuous control variables such as of PV outputs, but also handling discrete variables such as OLTC tap changes. In [20–22], a control method for coordinating the operation of OLTC and distributed generations (DGs) based on the initial optimal power flow (OPF) calculation in order to maintain the load end voltage of the feeder within the allowed band. The authors of [23,24] incorporated a semi-definite power flow relaxation to tackle such complex problems, while [25,26] decomposed the problem into subproblems by Benders decomposition method and alternate direction method of multipliers respectively. In [27–30], the discrete variables in optimization models are relaxed into continuous variables and then rounded to close integers. However, these solutions are the static optimization results, regardless of the strong time coupling between the adjustments of different devices. The authors in [31] proposed a two-stage dynamic coordination dispatch method based on the Haar wavelet transform to adjust the OLTC tap position and the reactive power of distributed generation. [32] implemented another two-stage dynamic reactive power dispatch method, which first performed a day-ahead dispatch plan for switched capacitor banks and OLTCs by Heuristic search, and then recalibrated the intra-day dispatch results of PVs. These two-stage methods mentioned pre-optimize discrete devices in advance without considering the interaction between OLTC tap changes and PV outputs. Consequently, the pre-planned scheduling may have large errors and lose dynamic optimality.

Furthermore, previous research has drawn attention to the solutions of PV generation uncertainties. In fact, most optimal dispatch methods based on the predicted scenario can only work in shorter periods, since accurate weather and load forecasts are only valid for a limited period in advance. A multi-step optimization method based on the model predictive control (MPC) principle has been verified to be well suited for this issue by determining the appropriate prediction horizon and control horizon [33,34]. Solving the rolling optimization problems of specific horizons can achieve a dynamic transition from the measured to the target values, which is different from single step optimizations. Notably, varying the horizon of prediction and control has a significant impact on the optimal operation of the current time window. The authors in [35] developed a planning method that leverages MPC principle to decide the optimal location and size of storage devices in ADN. [36] proposed a control strategy based on MPC to balance the intermittency of PV outputs by little adjustments of conventional generation and load, as well as the storage devices. In [9], an MPC-based corrective control is utilized to correct voltages out of limits by solving the OLTC voltage set-point and PV outputs. However, due to the different operation characteristics of various devices, the requirement of subdividing the control horizon was ignored. On the one hand, limited forecasts cannot support the long-period scheduling. On the other hand, frequent short horizons will increase the modeling time and make the optimization problem computationally intractable. Table 1 gathers the main features of ADN optimization methods found in the existing literature.

Table 1. Summary of the literature related to ADN optimization method.

Devices	Reference	Method/Algorithm	Remarks
OLTC	[7]	Mixed integer nonlinear programming (MINP)	• Disadvantages: due to physical constraints and low cost benefit ratios, OLTC cannot change flexibly to achieve real-time adjustment
DG	[12,13]	Decentralized control based on voltage sensitivity	• Advantages: The continuous, quick and frequent reactive power outputs of DGs avoids adding extra voltage devices and reactive compensators. • Disadvantages: DG reactive outputs are limited by capacity and power factor. It is insufficient to correct serious violations by DGs alone.
	[15]	A multi-mode adaptive local control method based on Q(P) characteristics	
	[16]	a combination of centralized remote control and local decentralized control	
DG, OLTC	[20–22]	Optimal power flow (OPF) calculation	• Disadvantages: These solutions are the static optimization results, regardless of the strong time coupling between the adjustments of different devices.
	[23,24]	Semi-definite relaxation	
	[25,26]	Benders decomposition	
	[27–30]	Relaxing discrete variables into continuous variables and rounding to close integers.	
	[31,32]	Two-stage dynamic coordination dispatch	• Advantages: the dynamic optimization results. • Disadvantages: The pre-planned scheduling may have large errors and lose dynamic optimality.
Storage device, OLTC, DG	[9,35,36]	Model predictive control (MPC)	• Advantages: Rolling optimization of the specific horizon can achieve a dynamic transition from the measured to the target values. • Disadvantages: The requirement of subdividing the control horizon for different devices is ignored.

In this paper, a decoupling rolling multi-period (DRM) reactive power and voltage optimization method of ADN is proposed. The main contribution is two-fold. First, for the mixed-integer reactive power and voltage optimization problem, we utilize Benders decomposition algorithm to decouple the coordination between discrete OLTC tap changers and continuous PV power outputs in the original problem into the master problem and the subproblem. In terms of time, our method designs the master problem of OLTC tap as a long-period optimization model, and the subproblem of PV power is a series of short-period optimization models. This allows us to address PV and load uncertainty by dividing the fluctuating PV and load condition into various short-period scenarios, avoiding frequent OLTC tap changes. Secondly, these short-period independent subproblems are incorporated into the MPC strategy and solved on a rolling basis, because predicting PV power generation of all short periods in the current time window may lead to large errors and additional adjustment costs. Based on the linearized voltage prediction model, the interrelation between rolling subproblems are considered to realize the gradual evolution of the ideal voltage in a long period, i.e., the prediction and control horizon of MPC. Besides, we present how to formulate Benders decomposition algorithm for this reactive power and voltage optimization problem, including the solution process, achieving the multi-period decoupling rolling optimization effect of different devices.

The rest of the paper is organized as follows: In Section 2, the model of voltage sensitivity is established, as well as the modeling of OLTC and PV. In Section 3, the proposed DRM architecture is illustrated. Section 4 formulates the decomposed optimization models and provides the solution process. In Section 5, the simulation results on the distribution test system are presented to validate the proposed strategy. The conclusions are drawn in Section 6.

2. Modeling of Active Distribution Network

2.1. Sensitivity between Node Voltage and Power

In order to discuss the influence of different voltage regulation devices on nodal voltages, the distribution network can be locally linearized to calculate the sensitivity model (the relationship between nodal voltage deviations and output changes of regulation devices) [37].

Assuming that a distribution network system contains n nodes, the voltage of Node i are expressed in polar coordinate form, $\dot{V}_i = V_i e^{j\theta_i} = V_i(cos\theta_i + jsin\theta_i)$. The modified Newton Raphson power flow equation can be simplified as:

$$\begin{bmatrix} \Delta \boldsymbol{P} \\ \Delta \boldsymbol{Q} \end{bmatrix} = -\boldsymbol{J}\begin{bmatrix} \Delta \boldsymbol{\theta} \\ \Delta \boldsymbol{V} \end{bmatrix} \tag{1}$$

where $\boldsymbol{V}$ is the diagonal matrix of voltage amplitude, $\boldsymbol{V}$ = diag(v_1, v_2, … , $v_{n\text{-}1}$), $\Delta\boldsymbol{\theta}$ and $\Delta\boldsymbol{V}$ are the corrections of the voltage phase angle and voltage amplitude respectively. The Jacobian matrix $\boldsymbol{J}$ is as follows:

$$\boldsymbol{J} = -\begin{bmatrix} \boldsymbol{H} & \boldsymbol{N} \\ \boldsymbol{K} & \boldsymbol{L} \end{bmatrix} = \begin{bmatrix} \boldsymbol{V} & \\ & \boldsymbol{V} \end{bmatrix}\left\{\begin{bmatrix} \boldsymbol{B}cos\theta & -\boldsymbol{G}cos\theta \\ \boldsymbol{G}cos\theta & \boldsymbol{B}cos\theta \end{bmatrix} - \begin{bmatrix} \boldsymbol{G}cos\theta & \boldsymbol{B}sin\theta \\ -\boldsymbol{B}cos\theta & \boldsymbol{G}sin\theta \end{bmatrix}\right\}\begin{bmatrix} \boldsymbol{V} & \\ & \boldsymbol{V} \end{bmatrix} \tag{2}$$

where $\boldsymbol{B}cos\boldsymbol{\theta}$ can be expressed as Equation (3) and the structures of other terms $\boldsymbol{B}\sin\boldsymbol{\theta}$, $Gcos\theta$, and $\boldsymbol{G}sin\boldsymbol{\theta}$ are similar.

$$\boldsymbol{B}cos\boldsymbol{\theta} = \begin{bmatrix} B_{1,1}cos\theta_{1,1} & \cdots & B_{1,j}cos\theta_{1,j} & \cdots & B_{1,j}cos\theta_{1,n} \\ \vdots & \ddots & \vdots & & \vdots \\ B_{i,1}cos\theta_{i,1} & \cdots & B_{i,j}cos\theta_{i,j} & \cdots & B_{i,n}cos\theta_{i,n} \\ \vdots & & \vdots & \ddots & \vdots \\ B_{n,1}cos\theta_{n,1} & \cdots & B_{n,j}cos\theta_{n,j} & \cdots & B_{n,n}cos\theta_{n,n} \end{bmatrix} \tag{3}$$

In the distribution network, the value of θ_{ij} is extremely small, and hence Equation (1) can be further simplified:

$$\begin{bmatrix} \boldsymbol{B}+\boldsymbol{Q} & -\boldsymbol{G}-\boldsymbol{P} \\ \boldsymbol{G}-\boldsymbol{P} & \boldsymbol{B}-\boldsymbol{Q} \end{bmatrix}\begin{bmatrix} \boldsymbol{V}\Delta\boldsymbol{\theta} \\ \Delta\boldsymbol{V} \end{bmatrix} = \begin{bmatrix} \Delta\boldsymbol{P}/\boldsymbol{V} \\ \Delta\boldsymbol{Q}/\boldsymbol{V} \end{bmatrix} \tag{4}$$

where $\boldsymbol{P}$ and $\boldsymbol{Q}$ are diagonal matrices, and their diagonal elements are P_i/V_i^2 and Q_i/V_i^2 respectively. Using the Gaussian elimination method for Equation (4), the sensitivity of nodal voltages and injected power can be calculated as:

$$\Delta\boldsymbol{V} = \Big((\boldsymbol{B}+\boldsymbol{Q})(\boldsymbol{G}-\boldsymbol{P})^{-1}(\boldsymbol{B}-\boldsymbol{Q}) + (\boldsymbol{G}+\boldsymbol{P})\Big)^{-1}\Delta\boldsymbol{P} \tag{5}$$

$$\Delta\boldsymbol{V} = -\Big((\boldsymbol{G}-\boldsymbol{P})(\boldsymbol{B}+\boldsymbol{Q})^{-1}(\boldsymbol{G}+\boldsymbol{P}) + (\boldsymbol{B}+\boldsymbol{Q})\Big)^{-1}\Delta\boldsymbol{Q} \tag{6}$$

Therefore, the active-voltage sensitivity and reactive-voltage sensitivity can be obtained:

$$\boldsymbol{S}_P = \Big((\boldsymbol{B}+\boldsymbol{Q})(\boldsymbol{G}-\boldsymbol{P})^{-1}(\boldsymbol{B}-\boldsymbol{Q}) + (\boldsymbol{G}+\boldsymbol{P})\Big)^{-1} \tag{7}$$

$$\boldsymbol{S}_\mathrm{Q} = -\Big((\boldsymbol{G}-\boldsymbol{P})(\boldsymbol{B}+\boldsymbol{Q})^{-1}(\boldsymbol{G}+\boldsymbol{P}) + (\boldsymbol{B}+\boldsymbol{Q})\Big)^{-1} \tag{8}$$

2.2. Modeling of OLTC

The discussed OLTC acts on the voltage set-point of the secondary side by changing the tap position. The sensitivity $\partial\boldsymbol{V}/\partial V_{tap}$ between nodal voltages and OLTC set-point can be approximated from the solution of two power flow runs with a single tap position difference [9], as follows:

$$\boldsymbol{S}_{tap} = \frac{\partial\boldsymbol{V}}{\partial V_{tap}} \approx \frac{\partial\Delta\boldsymbol{V}}{\partial\Delta V_d} \tag{9}$$

where ΔV_d is voltage variation on the low-voltage side after a OLTC tap change.

2.3. Modeling of PV

In this paper, PVs are set to adjust the reactive power output in the maximum power point tracking (MPPT) mode [7]. The maximum reactive power is limited by active power, power factor and capacity:

$$\begin{cases} Q_{m,PV}^{t,max} = P_{m,PV}^{t} tan\varphi_{max}, 0 < P_{m,PV}^{t} < P_l \\ Q_{m,PV}^{t,max} = \sqrt{(S_{m,PV})^2 - \left(P_{m,PV}^{t}\right)^2}, P_l < P_{m,PV}^{t} < P_{max} \end{cases} \tag{10}$$

$$P_l = S_{m,PV} cos\varphi_{max} \tag{11}$$

where, $P_{m,PV}^{t}$ is the *PV-m* active power output. $Q_{m,PV}^{t,max}$ is the maximum reactive power. $S_{m,PV}$ is the capacity of the *PV-m*, and φ_{max} is the maximum power factor angle.

3. Decoupling Rolling Multi-Period Architecture

In view of nodal voltage deviations caused by the high proportion of PV generation, the practical implementation is to adjust the OLTC tap positions and the active/reactive power outputs of distributed PVs. The OLTC tap changes are discrete, while the PV power outputs can continuously, quickly, efficiently and accurately respond to operation instructions. The DRM strategy focuses on the temporal interaction between PV and OLTC and explores their cooperation performance on voltage optimization.

The reactive power and voltage optimization model is a MINP problem. The Benders decomposition method is a distributed algorithm that decomposes the original MINP problem into the master problem and the subproblem to obtain the optimal operation results of different controllable devices in the same time step, as shown in Figure 1a. Due to the limitation of OLTC tap changes, the synchronized optimization framework cannot take full advantage of PV flexibility potential. The improved strategy in Figure 1b further decomposes the long-period subproblem of PV reactive power into multiple short-period problems, not only realizing rapid adjustment of PV reactive power, but also avoiding excessive and frequent OLTC tap changes. However, these parallel independent short-period subproblems of PV outputs are still based on the definite long-period PV power generation forecasts. Taking into account the uncertainty of PV power generation prediction, the prediction error becomes larger when the period is longer. The DRM method proposed in this paper rolls a series of short-period subproblems in the prediction horizon to smoothly adjust the PV power, as shown in Figure 1c.

The detailed DRM reactive power and voltage optimization strategy is shown in the Figure 2. The decomposed long-period master problem is to solve OLTC tap changes. Since the increasing number of tap actions will shorten the life of OLTC, the optimization function is to minimize the adjustment cost of OLTC and set at most one tap position change per long period to reduce frequent actions. The voltage is calculated by the sensitivity between the nodal voltage and the OLTC tap in Equation (9) to constrain the range of tap change. After the master problem is solved, the optimal solution of OLTC tap will be sent to subproblems for feasibility verification.

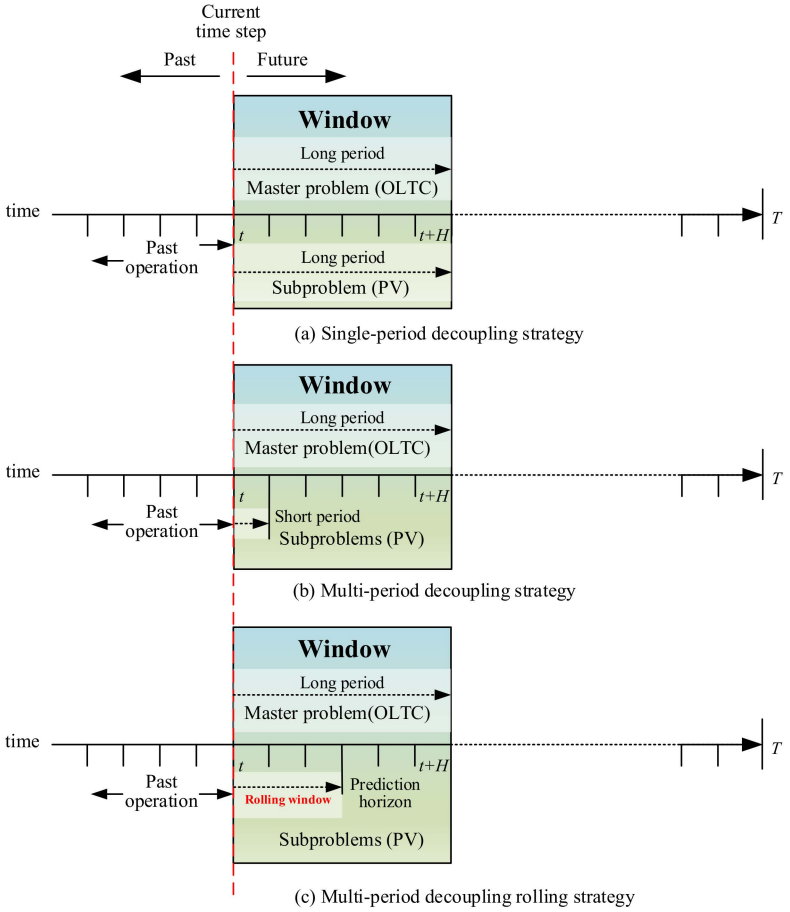

Figure 1. Comparison of the reactive power and voltage optimization strategy framework.

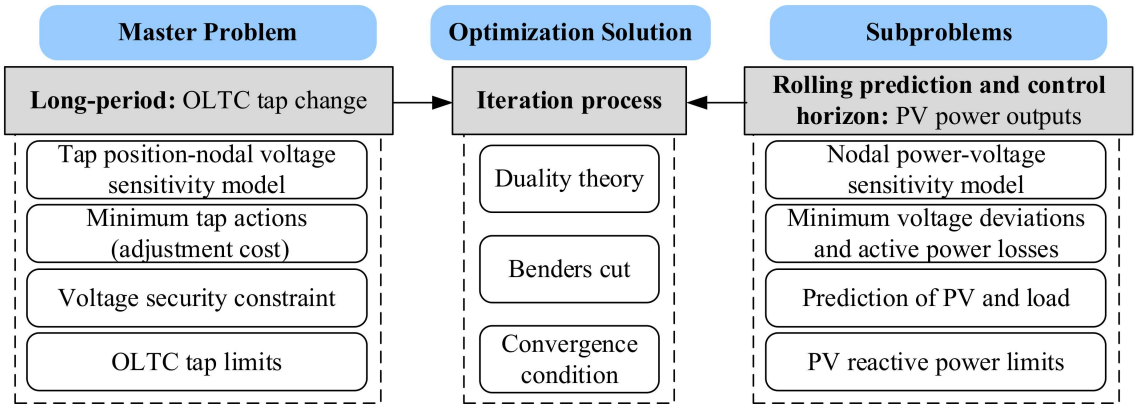

Figure 2. The detailed decomposition diagram of DRM strategy.

The subproblem is a series of PV active power and reactive power optimization problems of the prediction and control horizon considering the constraints of PV power factor and capacity. As the PV capacity limits the effectiveness of reactive power optimization, it is considered to reduce PV active power outputs in critical situations. Compared with the reactive power adjustment costs, the unit cost of PV active power regulation is significantly higher. Based on the MPC algorithm, a voltage prediction model is established from the sensitivity matrix of nodal power and voltage to ensure that the voltage is always in a safe range. Taking the current measured value as the initial state, the time window is rolled to complete the optimal solution in a long period, achieving a dynamic transition to

the ideal result and suppressing large fluctuations of the PV reactive power. The first short-period optimal set of PV reactive power instructions is issued and operated to minimize the sum of deviations between the future nodal voltages and the reference voltage.

Based on the iterative solution step of the Benders decomposition method, the global optimal solution of the DRM optimization model can be found [38]. After the master problem is solved, the OLTC tap position result is sent to the corresponding subproblems in the current time window, based on the duality theory. The subproblems implements rolling solution, which feedback the modified Benders cut constraint to the master problem, according to the feasibility verification. Then the master problem is re-solved by adding the new constraint from subproblems. In this way, the master problem and subproblem are iterated repeatedly until the convergence condition is satisfied and the optimal solution is obtained.

4. Reactive Power and Voltage Optimization Model

This section first establishes a common model of the ADN reactive power and voltage optimization problem, which is later decomposed in to the master problem and rolling subproblems according to the DRM method. At last, the solution process is introduced.

4.1. Objective Function

The objective function of the proposed DRM method is composed of three parts, which are the adjustment cost, the voltage deviation and the active power loss. Both OLTC and PV adjustment costs are considered in the objective function:

$$C_{tap} = c_b \Delta N_{tap}{}^2 \tag{12}$$

$$C_{PV} = c_{P,PV} \left\| \boldsymbol{P}_{PV} - \widetilde{\boldsymbol{P}}_{PV} \right\|_2^2 + c_{Q,PV} \left\| \Delta \boldsymbol{Q}_{PV} \right\|_2^2 \tag{13}$$

where $\boldsymbol{P}_{PV}$ and $\widetilde{\boldsymbol{P}}_{PV}$ are the actual output and predicted output of PV active power. ΔN_{tap} and $\Delta \boldsymbol{Q}_{PV}$ are the variations of OLTC tap and PVs reactive power respectively. c_b and c_{PV} are the unit cost coefficients of OLTC and PVs. Please note that the reactive power adjustment cost of PV is calculated by the PV reactive power output changes, while the PV active adjustment cost is the power loss caused by the PV active power curtailment when necessary.

The nodal voltage deviation is one of the most significant reliability factors and service quality indices [39,40], because it is harmful to the operation life and efficiency of electrical devices when the voltage deviation beyond a reasonable range. The fluctuations of load and PV generation increases the risk of node voltage exceeding the limit. However, considering the node voltage limit as a constraint may lead to the voltages rising to their maximum limits after optimization. Choosing the voltage deviations from the ideal voltage reference $\boldsymbol{V}^{ref}$ as an objective function can remove this problem, as shown in Equations (14). If the voltage deviation of the optimization result is large, the voltage is more likely to exceed the limit:

$$V_{sum,de} = \left\| \boldsymbol{V} - \boldsymbol{V}^{ref} \right\|_2^2 \tag{14}$$

Furthermore, distributed PV generation will affect the power flow direction and change the node voltages. This paper considers minimizing active power losses to improve the economy of ADN operation. The network active power loss can be obtained by:

$$P_{loss}^t = \sum_{i,j}^{N} G_{ij} \left(V_i^2 + V_i^2 - 2 V_i V_j \cos \theta_{ij} \right) \Delta t \tag{15}$$

In general, the objective function voltage optimization is established based on the chronological scenario:

$$J^* = \sum_{t_l=1}^{N_{T_l}} \left[c_b \Delta N_{tap}^{t_l\ 2} + \sum_{t_s=1}^{N_{T_s}} \left(c_{Q,PV} \left\| \Delta \boldsymbol{Q}_{PV}^{t_l,t_s} \right\|_2^2 + c_{P,PV} \left\| \boldsymbol{P}_{PV}^{t_l,t_s} - \widetilde{\boldsymbol{P}}_{PV}^{t_l,t_s} \right\|_2^2 + \left\| \boldsymbol{V}^{t_l,t_s} - \boldsymbol{V}^{ref} \right\|_2^2 + P_{loss}^{t_l,t_s} \right) \right] \tag{16}$$

where t_l and t_s mean the long-period time window and rolling short-period time window, while N_{T_l} is the total number of long periods and N_{T_s} is the total short periods in a long period.

4.2. Constraints

Some following constraints are required to set in the ADN reactive power and voltage optimization model. First, based on the sensitivity model for voltage calculation in Section 1, voltage security of each node should be guaranteed. Besides, the PV reactive power output cannot exceed its configured maximum range. Similarly, the OLTC tap is limited by its maximum tap position, as well as the restriction on tap changes of one action.

4.2.1. Voltage Constraints

The nodal voltages of each short period V^{t_l,t_s} can be estimated by the voltages in the previous period and the predicted variations in the current period with respect to OLTC tap changes $\Delta V_{tap}^{t_l,t_s}$ and PV and load power $\Delta \boldsymbol{V}_{PV,load}^{t_l,t_s}$, as shown in Equations (17) and (18). Then, the nodal voltages should be limited within a safe range:

$$\Delta \boldsymbol{V}_{tap}^{t_l,t_s} = \boldsymbol{S}_{tap} \Delta V_d \Delta N_{tap}^{t_l,t_s} \tag{17}$$

$$\Delta \boldsymbol{V}_{PV,load}^{t_l,t_s} = \boldsymbol{S}_P \left(\Delta \boldsymbol{P}_{PV}^{t_l,t_s} + \Delta \boldsymbol{P}_{load}^{t_l,t_s} \right) + \boldsymbol{S}_Q \left(\Delta \boldsymbol{Q}_{PV}^{t_l,t_s} + \Delta \boldsymbol{Q}_{load}^{t_l,t_s} \right) \tag{18}$$

$$\boldsymbol{V}^{t_l,t_s} = \boldsymbol{V}^{t_l,t_s-1} + \Delta \boldsymbol{V}_{tap}^{t_l,t_s} + \Delta \boldsymbol{V}_{PV,load}^{t_l,t_s} \tag{19}$$

$$V^{\min} \le \boldsymbol{V}^{t_l,t_s} \le V^{\max} \tag{20}$$

where $V^{\min}$ and $V^{\max}$ are the lower limit and upper limit of the voltage amplitude.$\Delta N_{tap}^{t_l,t_s}$ is the OLTC tap position change. $\Delta \boldsymbol{P}_{PV}^{t_l,t_s}$, $\Delta \boldsymbol{Q}_{PV}^{t_l,t_s}$, $\Delta \boldsymbol{P}_{load}^{t_l,t_s}$ and $\Delta \boldsymbol{Q}_{load}^{t_l,t_s}$ are the power variations of PV and load, which can be obtained as follows:

$$\begin{cases} \Delta N_{tap}^{t_l,t_s} = N_{tap}^{t_l,t_s} - N_{tap}^{t_l-1,t_s} & if t_s = 1 \\ N_{tap}^{t_l,t_s} = N_{tap}^{t_l,1} & if t_s \ne 1 \end{cases} \tag{21}$$

$$\begin{cases} \Delta \boldsymbol{P}_{PV}^{t_l,t_s} = \boldsymbol{P}_{PV}^{t_l,t_s} - \boldsymbol{P}_{PV}^{t_l,t_s-1} \\ \Delta \boldsymbol{Q}_{PV}^{t_l,t_s} = \boldsymbol{Q}_{PV}^{t_l,t_s} - \boldsymbol{Q}_{PV}^{t_l,t_s-1} \end{cases} \tag{22}$$

$$\begin{cases} \Delta \boldsymbol{P}_{load}^{t_l,t_s} = \boldsymbol{P}_{load}^{t_l,t_s} - \boldsymbol{P}_{load}^{t_l,t_s-1} \\ \Delta \boldsymbol{Q}_{load}^{t_l,t_s} = \boldsymbol{Q}_{load}^{t_l,t_s} - \boldsymbol{Q}_{load}^{t_l,t_s-1} \end{cases} \tag{23}$$

It is worth noting that the OLTC tap is only changed once in a long period, which is assumed to occur in the first short period, as in Equation (21). The PV active outputs and load conditions in Equations (22) and (23) are based on the current forecast.

4.2.2. PV Power Constraints

Due to the limitations of PV operation mode and capacity in Equations (10) and (11), the reactive adjustment constraint is:

$$\begin{cases} \boldsymbol{P}_{PV}^{\min} \le \boldsymbol{P}_{PV}^{t_l,t_s} \le \boldsymbol{P}_{PV}^{\max} \\ \boldsymbol{Q}_{PV}^{\min} \le \boldsymbol{Q}_{PV}^{t_l,t_s} \le \boldsymbol{Q}_{PV}^{\max} \end{cases} \tag{24}$$

where $\boldsymbol{Q}_{PV}^{\max}$ and $\boldsymbol{Q}_{PV}^{\min}$ are the reactive power up-limit matrix and down-limit matrix. $\boldsymbol{P}_{PV}^{\min}$ and $\boldsymbol{P}_{PV}^{\max}$ are the active power up-limit matrix and down-limit matrix.

4.2.3. OLTC Tap Constraints

The OLTC tap range as a key parameter should be considered, as well as the amplitude of one tap change:

$$N_{tap}^{\min} \le N_{tap}^{t_l} \le N_{tap}^{\max} \tag{25}$$

$$\Delta N_{tap}^{t_l} \in \{0, \pm 1\} \tag{26}$$

where $N_{tap}^{\max}$ and $N_{tap}^{\min}$ are the lower limit and upper limit of the OLTC tap position.

4.3. Model Decomposition

In this section, the Benders decomposition method is used to decompose the original optimization problem into a master problem and several MPC-based rolling subproblems to achieve the decoupling of different action periods, as well as the decoupling of discrete and continuous control variables.

(1) MPC-Based subproblem

The rolling subproblems are based on the MPC algorithm to solve the optimization problem of short-period continuous control variables, PV active and reactive power outputs. We set a predictive and control horizon consisting of H_s short periods. According to load and PV forecasts in the prediction and control horizon, the optimal operation sequence of PV power outputs can be obtained. The specific subproblem model solved by the k-th iteration is:

$$\begin{aligned} &J_{sub}^{t_l,k}\left(\Delta N_{tap}^{t_l,k}\right) = min \sum_{t_s=1}^{N_{Ts}} \left(\sum_{h_s=1}^{H_s} c_{Q,PV} \|\Delta \boldsymbol{Q}_{PV}^{t_l,t_s}\|_2^2 + c_{P,PV} \|\boldsymbol{P}_{PV}^{t_l,t_s} - \widetilde{\boldsymbol{P}}_{PV}^{t_l,t_s}\|_2^2 + \|\boldsymbol{V}^{t_l,t_s,hs} - \boldsymbol{V}^{ref}\|_2^2 + P_{loss}^{t_l,t_s} \right) \\ &S.T. \begin{cases} \Delta N_{tap}^{t_l} = \Delta N_{tap}^{t_l,k} : \lambda^k \\ Equations(17-20), (22,23) \\ Equations(10), (11), (24) \end{cases} \end{aligned} \tag{27}$$

where λ^k is a dual variable generated by constraint ($\Delta N_{tap}^{t_l} = \Delta N_{tap}^{t_l,k}$), which means that the result $\Delta N_{tap}^{t_l}$ of the k-th master problem is used as a parameter when the subproblem is solved.

(2) Master Problem

The long-period master problem considers the adjustment cost of OLTC and retains the discreteness of the control variable, the OLTC tap. The objective function is to minimize the adjustment cost caused by OLTC tap changes. The master problem is expressed as:

$$\begin{aligned} &J_m^{t_l,k+1}\left(J_{sub}^{t_l,k}, \Delta N_{tap}^{t_l,k}, \lambda^k\right) = \min c_b \Delta N_{tap}^{t_l\ 2} + \alpha \\ &S.T. \begin{cases} J_{sub}^{t_l,k} + \lambda^k \left(\Delta N_{tap}^{t_l} - \Delta N_{tap}^{t_l,k}\right) \le \alpha \\ \alpha \ge \alpha_{down} \\ \text{Equations} \quad (19), (21) \end{cases} \end{aligned} \tag{28}$$

The first line of the constraints is the form of Benders cut, where α is an auxiliary variable. α_{down} is a sufficiently small positive number used as a substitute for the objective function value of the subproblem when the master problem is solved for the first time, i.e., k = 1. Afterwards, the master problem is re-solved according to the new constraints in each iteration.

4.4. Solution Algorithm

In this paper, the global optimal solution is obtained through multiple iterations between the master problem and subproblems. The detailed solution process based on Benders decomposition algorithm is shown in Figure 3.

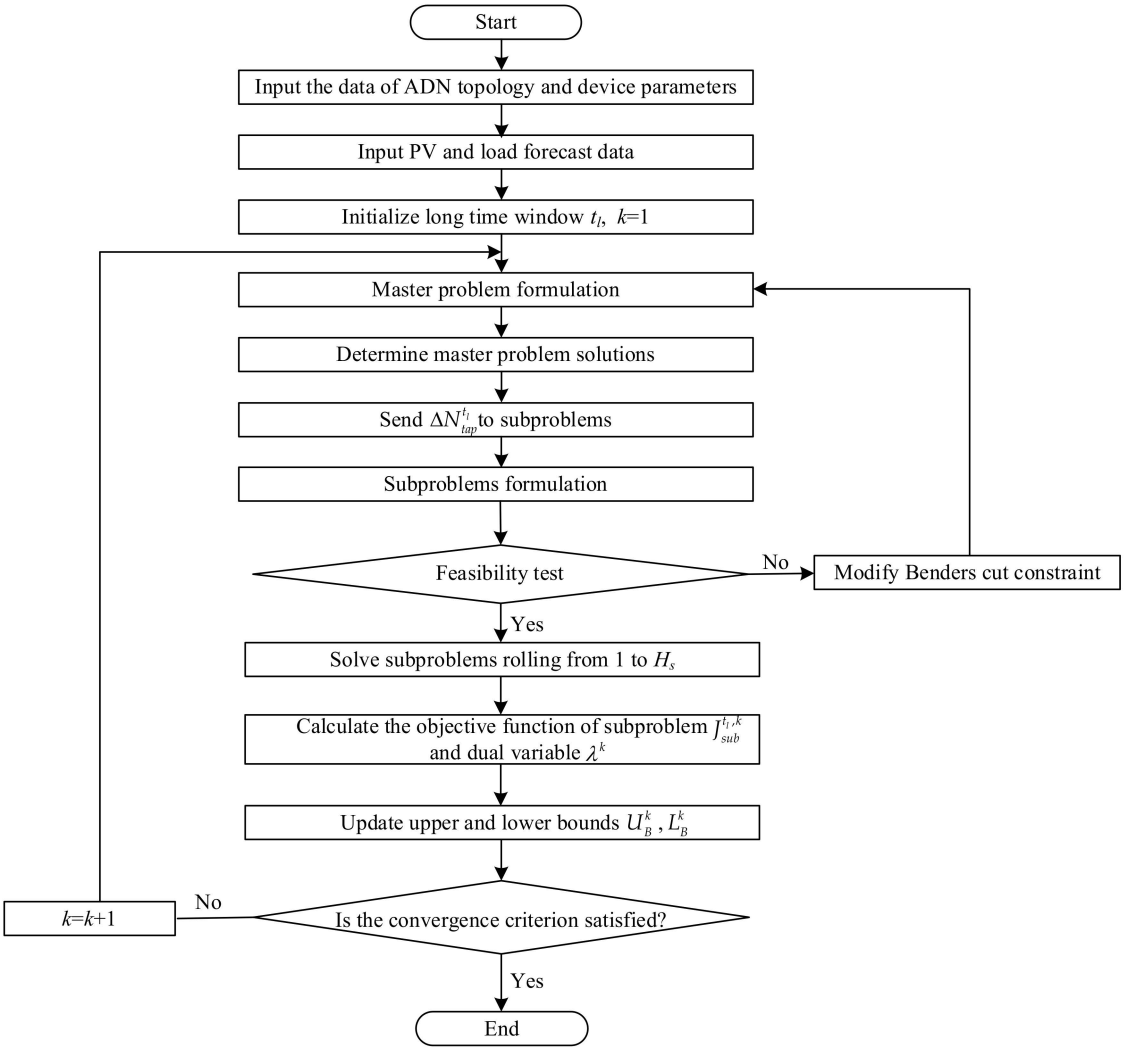

Figure 3. Flowchart of the proposed DRM strategy to solve the reactive power and voltage problem.

After collecting the parameters and forecasts in the optimization model, initialization is required to enter the Benders loop. The master problem in Equation (28) of OLTC tap position is first solved, and the lower bound L_B^k of the original problem is updated according to Equation (29). Then, the result of the master problem is substituted into subproblems for feasibility test. If the OLTC tap result satisfies the constraints, the subproblems in Equation (27) are continued to be solved, and the upper bound U_B^k is updated according to Equation (30). If not, the Benders cut constraint is modified to re-solve the master problem. When the difference between the upper bound and the lower bound is less than the threshold ε in Equation (31), the global optimal solution of the original problem has been found, otherwise the loop needs to be entered again:

$$L_B^k = c_b \Delta N_{tap}^{t_l\ 2} + \alpha^k \tag{29}$$

$$U_B^k = J_{sub}^{t_l,k} + c_b \Delta N_{tap}^{t_l\ 2} \tag{30}$$

$$\left| \frac{U_B^k - L_B^k}{U_B^k} \right| \leq \varepsilon \tag{31}$$

5. Results and Discussion

5.1. Simulation Results of Case 1

A modified PG&E 69-bus distribution network in Figure 4 with specific configurations in Table 2 is selected to test the optimization algorithms performance. More detailed topology information can be obtained by referring to [41]. Figure 5 shows the forecasted aggregate power profile of PV and total daily load profile. The example simulation models are implemented in the MATLAB R2018b environment, and the optimization problems are solved by a commercial solver Gurobi8.9.0 [42]. The upper and lower levels of voltage are 1.05 p.u. and 0.95 p.u. of its base value [43]. The minimum power factor of PV is set to 0.95. Moreover, the unit cost coefficient of OLTC tap is \$6 [44] and the upper limit for the daily OLTC tap is set to 20 changes [45,46]. The estimated unit cost coefficient of PV active power and reactive power output are 0.8\$/MW and 0.1\$/MVar [47] for the economy estimation.

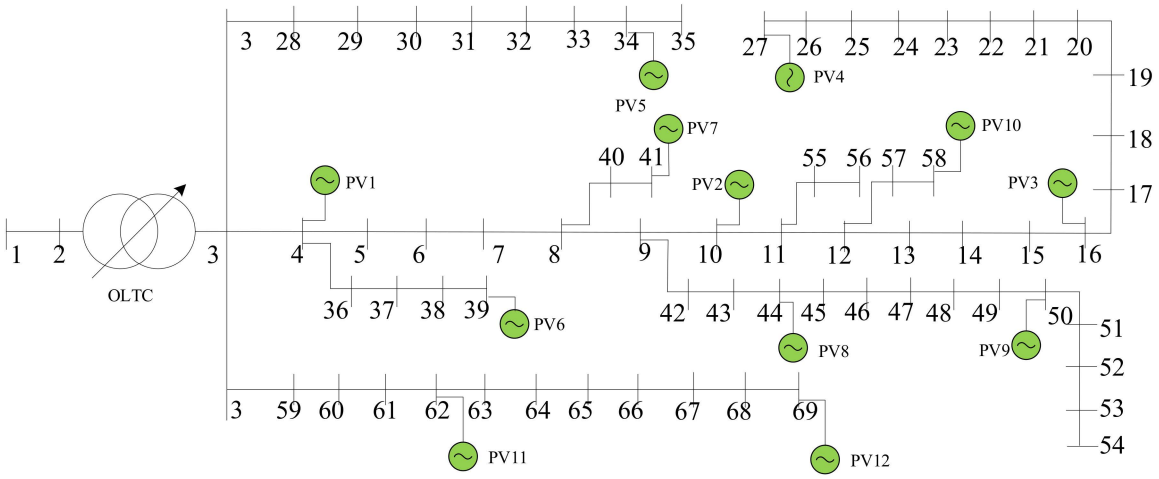

Figure 4. Modified PG&E 69-bus system with PVs.

Table 2. The basic installation parameters of OLTC and PVs.

Devices	Parameters	Values
OLTC	Tap range	−8–8
PV	Capacity	500 kWP

To verify the advantages of the proposed DRM strategy, two other strategies were investigated to compare and analyze the performance in different cases, namely: single-period decoupling strategy (S1) and multi-period decoupling and non-rolling strategy (S2). The strategies are illustrated in Figure 1a,b. Table 3 further presents the differences between them in detail.

Table 3. Comparison of three voltage optimization strategies.

Characteristic	S1	S2	DRM
Decoupling of discrete/continuous device actions	√	√	√
Subdividing optimization periods	×	√	√
MPC-based rolling optimization	×	×	√

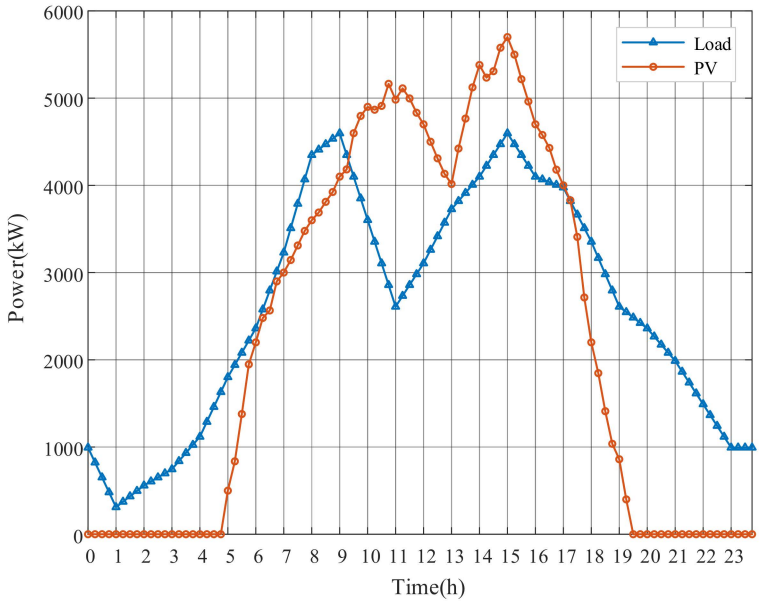

Figure 5. The aggregate daily load profile and solar power profile of Case 1.

5.1.1. Optimal Results

This paper takes 11:00 and 24:00 results as examples to represent voltage deviations of the proposed DRM strategy, as shown in Figure 6. Although some nodes near the end of feeders appear overvoltage (over 1.05 p.u.) at 11:00 due to the high PV outputs, the nodal voltages return to the safe state after optimization. For the result of 24:00 without PV generation, it not only shows that each feeder has a voltage drop due to line impedance, but also illustrates the whole ADN operates within the acceptable range. The optimized overall voltage level is closer to the reference value. The voltage deviation of the Node 16 and Node 54 for a day are shown in Figure 7. The proposed DRM strategy can greatly reduce the voltage amplitudes by adjusting OLTC tap changes and PV reactive power outputs. It is worth noting that Node16, the grid-connected point of PV3, severely exceeded the upper limit at around 11:00, and the voltage drop after optimization is more obvious than that of Node 54.

Figures 8–10 show the optimal operation results of OLTC tap and PV power outputs after adopting the DRM strategy. When PV generation is excessive, OLTC raises the tap to reduce the substation secondary side voltage, whereas PVs absorb reactive power to regulate voltages of the surrounding nodes. Remarkably, at around 11:00, even though the voltage has exceeded the limit, the OLTC tap is not further changed, while the active power output of PV4 in Figure 10 is reduced at noon to decrease the voltage level, due to the limited reactive power capacity. The results indicate that the adjustment of PV output can be used to address local voltage problems in feeders. However, because of the limited solar radiation in the morning from 1:00 to 6:00, PV generation is nonexistent. The OLTC tap can only be used to stabilize the voltage level. The numerical results of DRM strategy have been presented in Appendix A for this paper.

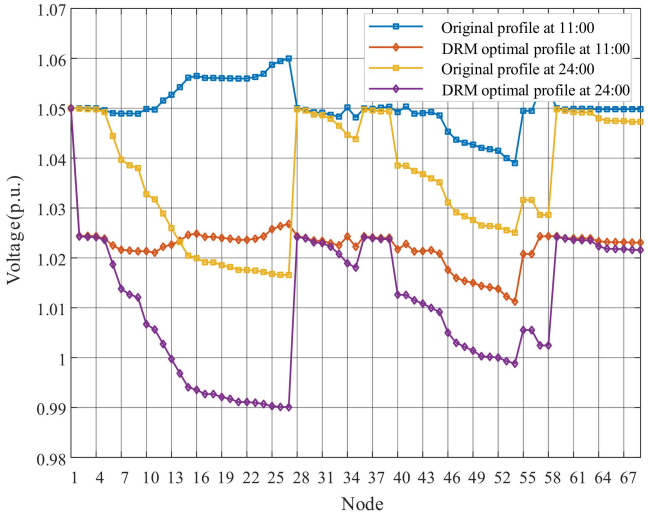

Figure 6. The nodal voltages of 11:00 and 24:00.

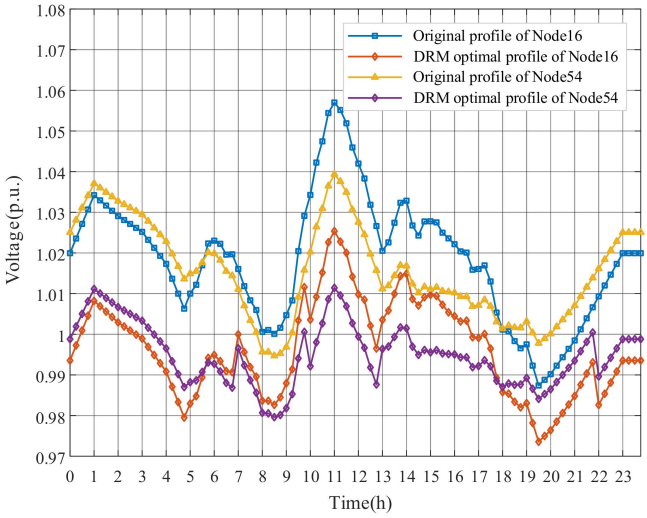

Figure 7. The daily voltages of Node16 and Node54.

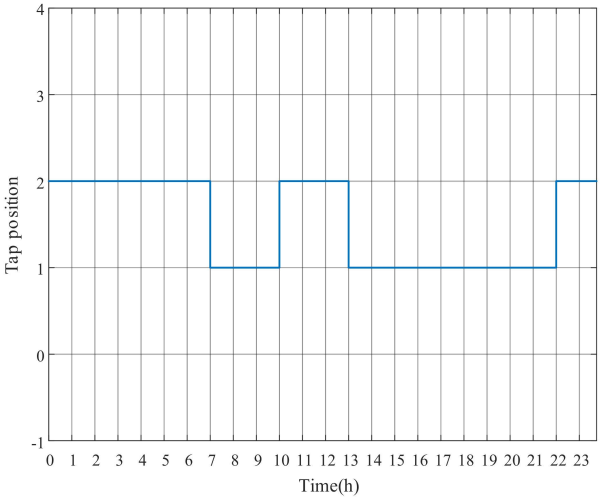

Figure 8. OLTC tap changes with DRM strategy.

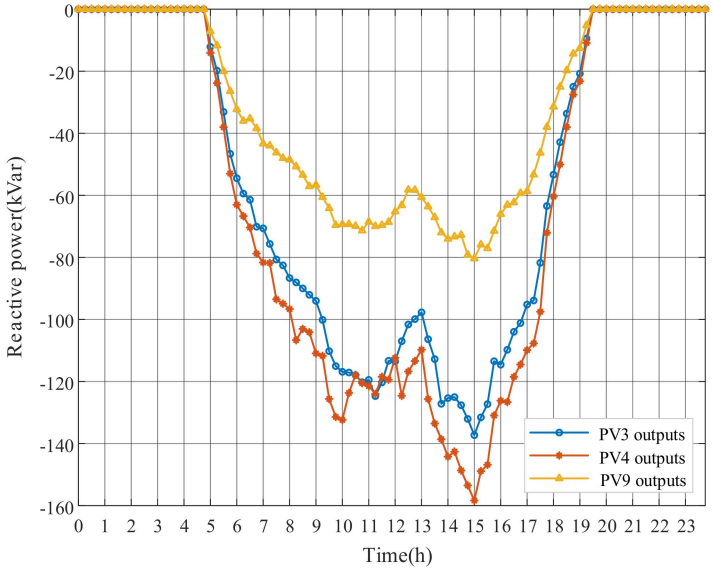

Figure 9. PV reactive power outputs with DRM strategy.

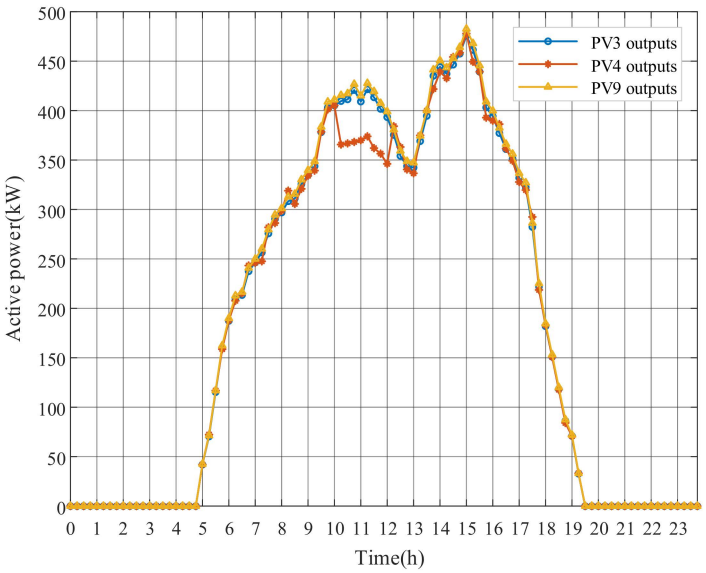

Figure 10. PV active power outputs with DRM strategy.

5.1.2. Performance Comparison

Adjustment Costs

PV reactive power outputs (for example, PV3) and OLTC tap actions of the three mentioned optimization strategies are shown in Figures 11 and 12, respectively. Since the master problems of OLTC in the three strategies are set within the same long period, the results and adjustment costs of OLTC tap is the same. Table 4 shows that the adjustment costs of S1 and S2 are much higher than that of DRM strategy, which is because of the differences in PV reactive power outputs. The long-period PV forecasts applied by S1 usually present uncertainties, which leads to large changes in PV reactive power outputs of neighbored long periods, and hence the adjustment costs increase significantly. Compared with DRM, S2 lacks the rolling optimization setting of MPC algorithm based on the prediction and control horizon. The optimization function of the rolling subproblems is to gradually reduce the difference between the current state and the ideal state in the long prediction and control horizon. A series of short-period PV reactive output instructions are obtained, although only the first short-period

instructions are executed. As shown in Figure 11, the PV reactive power results of several independent short-period subproblems in S2 fluctuate obviously, raising the adjustment costs of PVs, while the based-MPC DRM strategy indicates a significant reduction in cost.

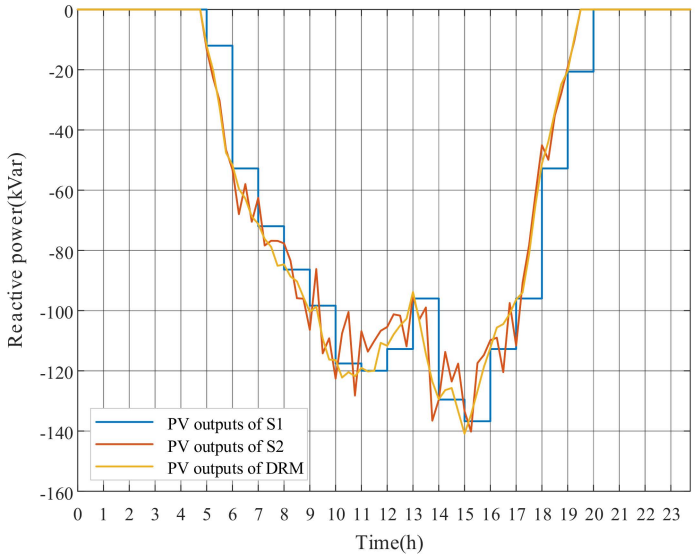

Figure 11. PV3 reactive power outputs with three strategies.

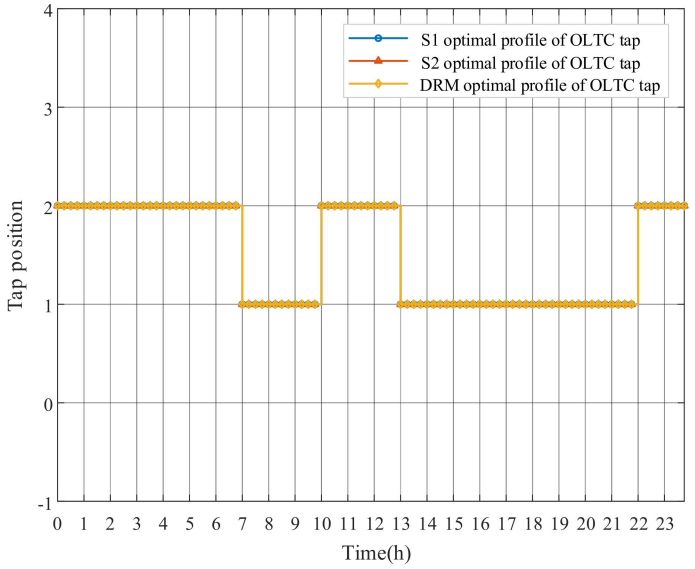

Figure 12. OLTC tap changes with three strategies.

Table 4. Adjustment costs of three strategies.

Adjustment Cost	S1	S2	DRM
OLTC	$24	$24	$24
PVs	$1.17	$1.64	$0.63
Total	$25.17	$25.64	$24.63

Voltage Deviations

In order to verify the superiority of the proposed DRM strategy in terms of voltage deviations, the voltage results at 11:00 and 24:00 from different strategies is shown in Figure 13. Three strategies

can effectively reduce the voltage level, the voltage amplitude of S1 is higher than that of S2 and DRM at 11:00. The voltage results of some nodes by S2 and DRM are similar, while the voltages of the feeder from Node 13 to Node 27 by S2 are higher than the DRM strategy. The difference between the three strategies does not exist at night, because PVs do not generate electricity.

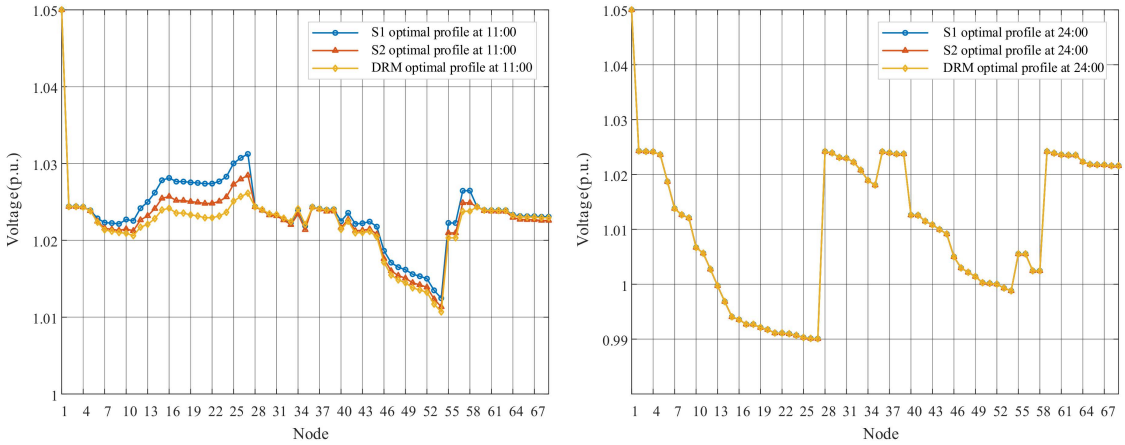

Figure 13. The nodal voltages of 11:00 and 24:00 from three strategies.

Figure 14 compares the daily voltages of Node 16 and Node 54 optimized by S1, S2 and DRM strategy from the perspective of time changes. The differences between S1 and DRM strategy are still existed, while the voltage results of S2 and DRM are similar. More accurate data are given in Table 5, which is also shows this phenomenon. For the all-day voltage deviations, compared with the original profile, the three optimization methods all achieve a voltage deviation reduction of more than 60%. The S1 voltage deviation is 0.88 p.u. more than that of the DRM due to the errors in the long-period PV forecasts, while the voltage deviation difference between S2 and DRM is 0.23 p.u.

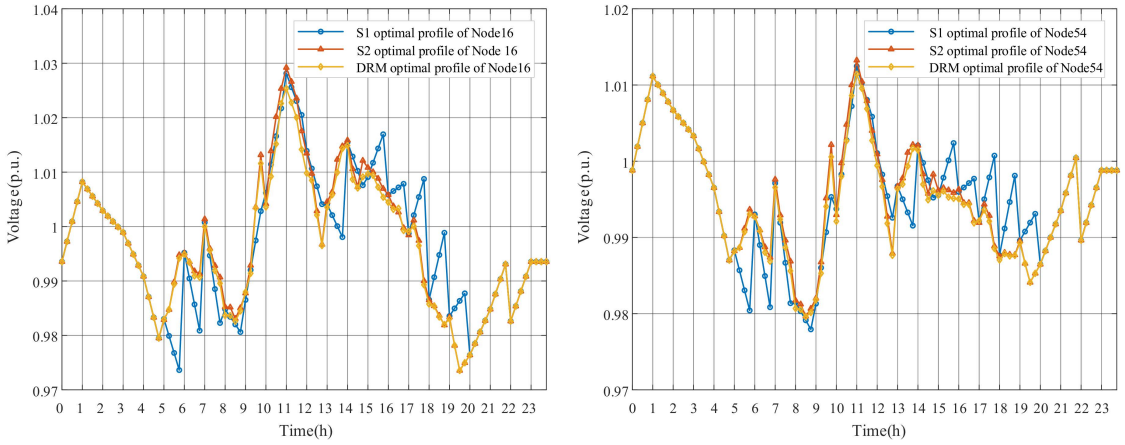

Figure 14. The daily voltages of Node16 and Node54 from three strategies.

Table 5. Voltage deviation results of three strategies.

	Original	S1	S2	DRM
All nodes at 11:00	3.4951 p.u.	1.6899 p.u.	1.6806 p.u.	1.5839 p.u.
All nodes at 24:00	2.4852 p.u.	0.9467 p.u.	0.9467 p.u.	0.9467 p.u.
Node 16 all day	1.9247 p.u.	1.0189 p.u.	1.0010 p.u.	0.9740 p.u.
Node 54 all day	1.5351 p.u.	0.6928 p.u.	0.6899 p.u.	0.6881 p.u.
All nodes all day	299.9501 p.u.	122.7256 p.u.	122.0783 p.u.	121.8496 p.u.

Active Power Losses

Table 6 shows the simulation results of the active power loss from the three strategies. Before PVs are connected to the distribution, the active power loss is as high as 4.8305 MWh a day. The distributed PV power generation can greatly reduce the network losses, only 2.0546 MWh. Due to the PV power transmission, the network loss results of the three optimization strategies are slightly higher than the original data. However, since some original nodal voltages exceed the upper limit, the voltage optimization strategy has to be implemented. Among the three strategies, S1 has the largest active power losses, because the forecast of load and PV power generation is uncertain, and the results of long-period strategy cannot achieve the dynamic optimization, resulting in a large amount of power loss. The active power loss of S2 considering different optimization periods is a little more than that of DRM strategy. The reason is that S2 is the static optimization method of each short period based on forecasts with errors, while the DRM strategy using dynamic real-time forecasts achieves the gradual approximation of the ideal value by rolling the time window.

Table 6. Active power losses from three strategies.

	No PV	**Original**	**S1**	**S2**	**DRM**
Active power losses	4.8305 MWh	2.0546 MWh	2.7143 MWh	2.6610 MWh	2.6472 MWh

Computation Time

The computation time of the three strategies is shown in Table 7. The present case only focuses on the differences in computation time caused by the optimization strategy, including modeling and solution, without considering the time spent on PV and load forecasting. Based on the 69-node distribution system configuration of Case 1 and the long period setting of S1, the 1-h daytime optimization result including OLTC tap and PV power requires 21.46 s, and the result of one day requires 5.33 min. Both S2 and the DRM strategy set the short optimization period about 15 min for PV output, and hence there are 96 changes in PV output per day. S2 takes 9.07 s to solve a short-period subproblem of PV power during the day. Since the linear sensitivity between node voltage and power is used instead of the nonlinear power flow constraints, although the optimization problems and variables have been increased by almost 4 times compared with S1, the computation time has only increased by around 2 times. The 1-h optimization requires 48.94 s, and the total computation time of one day is 11.64 min. The DRM strategy applies MPC algorithm to improve the subproblems of S2, and a short-period PV results by rolling optimization only increases by 1.36 s. The optimal results of 96 times a day takes 2.75 min longer than S2 in total. Comparing the computation time of a 1-h optimization, it can be seen that the computation time mainly depends on the number of iterations between master problems and subproblems, while the additional time required for rolling optimization of continuous PV outputs is not much. When the scale of the distribution network expands, the significant increase in nodes and discrete devices will result in more computation time.

Table 7. Computation time of three strategies.

	S1	**S2**	**DRM**
Long period (1 h) optimization	21.46 s	48.94 s	50.23 s
Short period (15 min) PV optimization	-	9.07 s	10.43 s
One day optimization	5.33 min	11.64 min	14.39 min

5.2. Simulation Results of Case 2

Compared with Case 1, Case 2 is a system configuration with uneven distribution of PVs, as shown in Figure 15. The feeder from Node 28 to Node 35 is completely passive and is not connected to any PV.

The parameters of each PV source and OLTC remain unchanged, in Table 2. The forecasted aggregate power profile of PV and total daily load profile are shown in Figure 16.

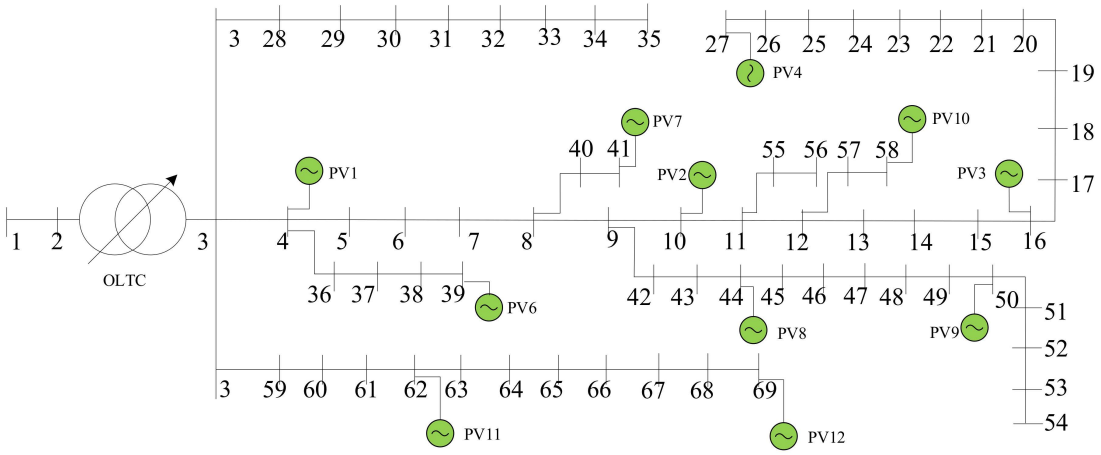

Figure 15. Modified PG&E 69-bus system with uneven PVs.

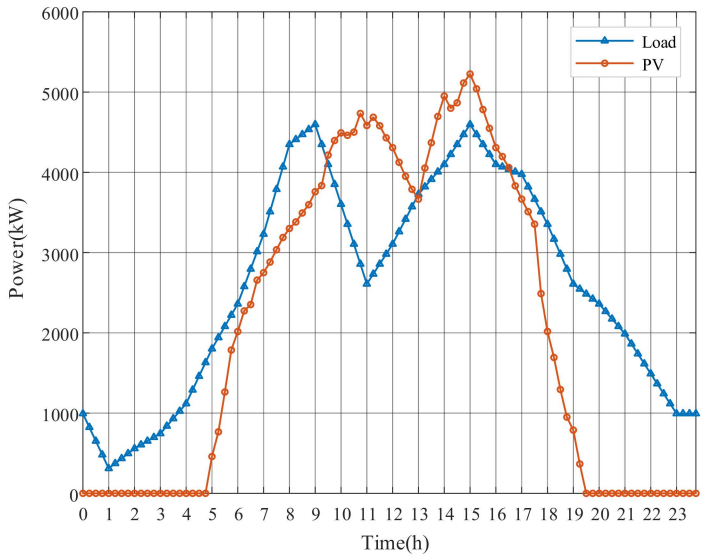

Figure 16. The aggregate daily load profile and forecasted PV power profile of Case 2.

The voltage results of all nodes at 11:00 and 24:00 are shown in Figure 17. The 11:00 voltage is significantly different from that of Case 1, and a slight overvoltage occurs in the system. In the original profile, the feeder voltage without PV connection from Node 28 to Node 35 gradually decrease due to the power loss caused by the line impedance. Compared with Case 1, the sum of original voltage deviations is smaller, and it is further reduced after optimization by DRM strategy.

Figure 18 reflects the differences in voltage changes at Node 27 and Node 35, the ends of two feeders. The voltage of Node 27 varies considerably, which is affected by the adjustment of the PV power on the feeder between Node 4 and Node 27. The Node 35 is only affected by load fluctuations and OLTC tap adjustments, and hence the changes are small.

The OLTC tap position and PV outputs of the DRM optimization strategy are shown in Figures 19–21. Compared with Figure 8 of Case 1, the number of OLTC tap changes is significantly decreased, because the original node voltages of Case 2 do not excessively exceed the upper limit. The frequent OLTC tap changes are avoided due to the impact of OLTC on the substation secondary bus voltage and its higher adjustment cost. We can see that DRM strategy mainly optimizes the voltage by adjusting PV outputs. In Figure 20, PV1 and PV4 absorb a large amount of reactive power to

decrease the voltage deviation. The reactive power absorption of PV9 at Node 50 is less because the end node voltage of the feeder is relatively low. From Figure 21, the PV active power outputs are still at the predicted level. It can be explained that PVs provide sufficient reactive power capacity at this time, avoiding the PV active power curtailment.

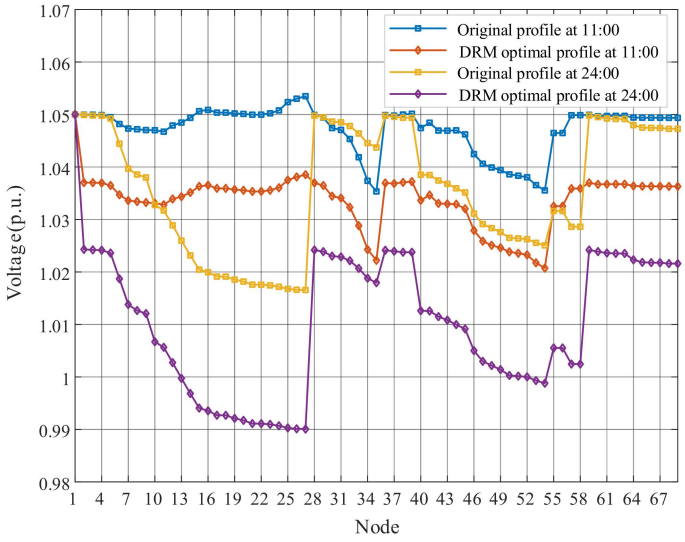

Figure 17. The nodal voltages at 11:00 and 24:00 of Case 2.

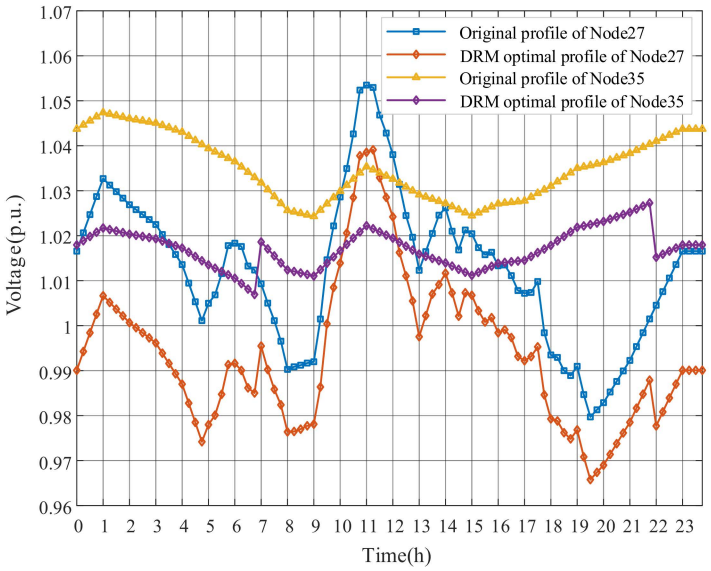

Figure 18. The daily voltages at Node27 and Node35 of Case 2.

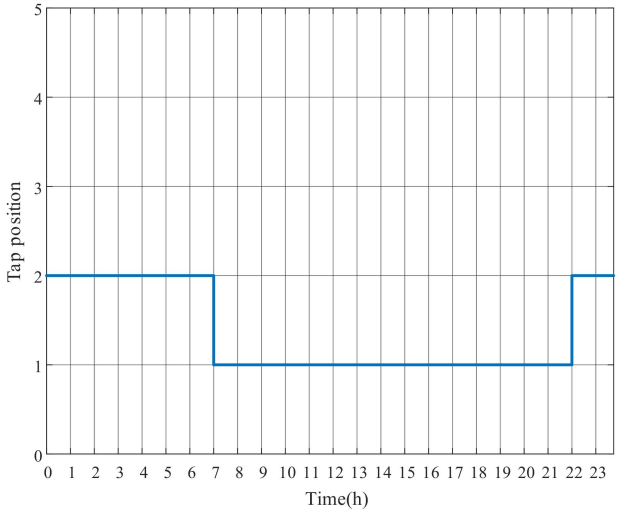

Figure 19. OLTC tap changes with DRM strategy of Case 2.

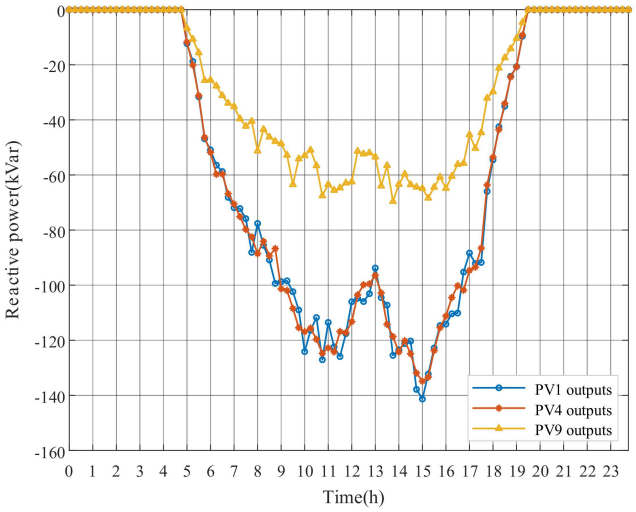

Figure 20. PV reactive power outputs with DRM strategy of Case 2.

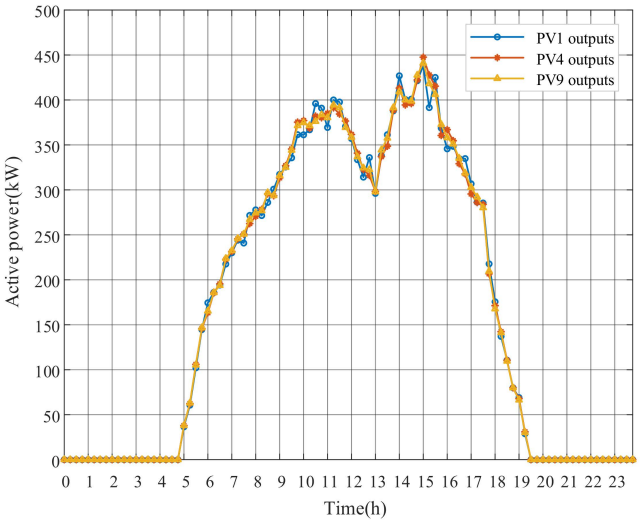

Figure 21. PV active power outputs with DRM strategy of Case 2.

6. Conclusions

In this paper, a novel DRM method is applied to the power and voltage optimization of ADN cooperating distributed PV and OLTC. According to the discrete and continuous characteristics of control variables, the proposed method utilizes a Benders decomposition algorithm to design a long-period master problem of OLTC tap and short-period subproblems of PV power outputs, achieving the decoupling of different devices actions. The different optimization time step considering the operation principles of devices not only avoids the frequent OLTC tap changes, but also further reduces voltage deviations caused by the stochastic intermittence and fluctuations of PV. The independent subproblems are then further modified into a series of rolling optimization models within long predictive and control horizons based on MPC algorithm considering the uncertainty of PV power generation and load. The rolling optimization of PV power achieves the gradual evolution of the ideal voltage in a long period without causing violent fluctuations in PV reactive power outputs, which greatly decreases adjustment costs. In the case study of the modified PG&E 69-node distribution network, the other two methods are compared to demonstrate the effectiveness and economy of DRM method. The future work would move forward to the implementation of the proposed optimization method considering the high uncertainty of renewable energy generation in large scale ADN. Besides, the impact of energy storage system on the dynamic voltage optimization is introduced. These issues would be established as subsequent research objectives.

Author Contributions: Conceptualization, X.G. and L.S.; methodology, L.S. and C.Z.; software, L.S.; validation, L.S., X.G. and P.L.; investigation, X.G.; resources, X.G.; data curation, C.Z.; writing—original draft preparation, L.S.; writing—review and editing, L.S.; supervision, X.D.; project administration, X.D. All authors have read and agreed to the published version of the manuscript.

Funding: This research was funded by the Science and Technology Program of State Grid Corporation of Zhejiang Province under Grand 5211DS17001Z.

Conflicts of Interest: The authors declare no conflict of interest.

Nomenclature

α	auxiliary variable
α_{down}	initial lower bound of α
λ	dual variable
$\boldsymbol{\theta}, \theta_i, i \in N$	nodal voltage phase angle
$\varphi_{\max}$	PV maximum power factor angle
$\boldsymbol{B}, \boldsymbol{G}$	set of conductance and susceptance
c_b	unit cost coefficients of OLTC
$c_{P,PV}$,$c_{Q,PV}$	unit cost coefficients of PV active power and reactive power
$\boldsymbol{H}, \boldsymbol{N}, \boldsymbol{K}, \boldsymbol{L}$	Elements in the Jacobian matrix
$\boldsymbol{J}$	Jacobian matrix from Newton Raphson power flow equation
J_{sub}, J_m	objective function of subproblems and the master problem
L_B^k, U_B^k	lower and upper bound of the original problem
k	number of iterations
$\boldsymbol{S}_P, \boldsymbol{S}_Q$	power-voltage sensitivity matrix
$N_{tap}, \Delta N_{tap}$	OLTC tap position and OLTC tap changes
$N_{tap}^{\max}$,$N_{tap}^{\min}$	lower and upper bound of OLTC tap position
$S_{m,PV}$	PV-m capacity
t_l	long-period time window
t_s	rolling short-period time window
N_{T_l}	total number of long periods
N_{T_s}	total number of short periods in a long period
$\boldsymbol{V}, V_i, i \in N$	nodal voltage amplitude
V_{tap}	OLTC set-point
ΔV_d	voltage variation on the low-voltage side after a OLTC tap change
$V^{\min}$,$V^{\max}$	lower and upper bound of nodal voltage amplitude

$\boldsymbol{P}, \boldsymbol{Q}$	set of nodal power and reactive power
$\boldsymbol{P}_{loss}$	active power loss
$\boldsymbol{P}_{load}, \boldsymbol{Q}_{load}$	set of load power
$\widetilde{\boldsymbol{P}}_{PV}$	set of PV predicted active power outputs
$\boldsymbol{P}_{PV}, \Delta\boldsymbol{P}_{PV}$	set of PV actual active power and active power changes
$\boldsymbol{Q}_{PV}, \Delta\boldsymbol{Q}_{PV}$	set of PV reactive power and reactive power changes
$\boldsymbol{Q}_{PV}^{\min}, \boldsymbol{Q}_{PV}^{\max}$	lower and upper bound PVs reactive power

Abbreviations

ADN	Active distribution network
DG	Distributed generation
DRM	Decoupling rolling multi-period
MINP	Mixed integer nonlinear programming
MPC	Model predictive control
MPPT	Maximum power point tracking
OPF	Optimal power flow
OLTC	On-load tap changer
PCC	Point of common coupling
PV	Photovoltaic

Appendix A

Table A1. Voltage results obtained by DRM strategy of Case 1 (p.u.).

Node	0:00	1:00	2:00	3:00	4:00	5:00	6:00	7:00
1	1.050000	1.050000	1.050000	1.050000	1.050000	1.050000	1.050000	1.050000
2	1.024297	1.024349	1.024331	1.024316	1.024288	1.024258	1.024293	1.036911
3	1.024204	1.024308	1.024271	1.024242	1.024185	1.024126	1.024196	1.036784
4	1.024148	1.024262	1.024221	1.024190	1.024127	1.024058	1.024125	1.036702
5	1.023609	1.023882	1.023783	1.023709	1.023558	1.023374	1.023472	1.035926
6	1.018692	1.021093	1.020227	1.019572	1.018249	1.016798	1.018217	1.029404
7	1.013801	1.018310	1.016683	1.015453	1.012969	1.010310	1.013207	1.023211
8	1.012651	1.017657	1.015851	1.014486	1.011728	1.008789	1.012057	1.021791
9	1.012083	1.017339	1.015443	1.014009	1.011114	1.008026	1.011448	1.021032
10	1.006702	1.014576	1.011735	1.009588	1.005249	1.000726	1.006185	1.014380
11	1.005641	1.014019	1.010997	1.008712	1.004095	0.999267	1.005026	1.012910
12	1.002728	1.012552	1.009009	1.006330	1.000915	0.995419	1.002733	1.010033
13	0.999731	1.011142	1.007028	1.003916	0.997623	0.991292	0.999968	1.006460
14	0.996840	1.009774	1.005111	1.001584	0.994450	0.987361	0.997493	1.003277
15	0.994061	1.008450	1.003264	0.999339	0.991401	0.983635	0.995319	1.000496
16	0.993544	1.008204	1.002920	0.998923	0.990834	0.982943	0.994916	0.999981
17	0.992702	1.007805	1.002362	0.998243	0.989909	0.981711	0.993817	0.998542
18	0.992692	1.007800	1.002355	0.998235	0.989898	0.981697	0.993805	0.998526
19	0.992104	1.007527	1.001968	0.997762	0.989252	0.980857	0.993138	0.997652
20	0.991726	1.007351	1.001720	0.997459	0.988836	0.980317	0.992709	0.997090
21	0.991114	1.007067	1.001318	0.996968	0.988165	0.979445	0.992017	0.996183
22	0.991098	1.007061	1.001308	0.996955	0.988147	0.979422	0.992005	0.996166
23	0.990971	1.007007	1.001228	0.996855	0.988006	0.979268	0.991994	0.996153

Table A1. *Cont.*

Node	0:00	1:00	2:00	3:00	4:00	5:00	6:00	7:00
24	0.990694	1.006891	1.001054	0.996637	0.987699	0.978932	0.991972	0.996124
25	0.990287	1.006732	1.000806	0.996321	0.987245	0.978513	0.992310	0.996566
26	0.990118	1.006666	1.000703	0.996190	0.987058	0.978340	0.992448	0.996748
27	0.990071	1.006648	1.000674	0.996154	0.987005	0.978325	0.992630	0.996990
28	1.024183	1.024294	1.024254	1.024224	1.024163	1.024097	1.024164	1.036745
29	1.023924	1.024122	1.024051	1.023997	1.023888	1.023744	1.023776	1.036263
30	1.023108	1.023808	1.023554	1.023363	1.022981	1.022483	1.022613	1.034712
31	1.022964	1.023752	1.023466	1.023252	1.022821	1.022260	1.022407	1.034438
32	1.022245	1.023475	1.023028	1.022693	1.022020	1.021146	1.021381	1.033068
33	1.020784	1.022891	1.022126	1.021552	1.020400	1.018958	1.019548	1.030635
34	1.018914	1.022164	1.020984	1.020098	1.018320	1.016368	1.018208	1.028856
35	1.018058	1.021818	1.020454	1.019428	1.017371	1.014905	1.016329	1.026352
36	1.024140	1.024256	1.024214	1.024182	1.024119	1.024049	1.024115	1.036691
37	1.023948	1.024097	1.024043	1.024002	1.023921	1.023823	1.023886	1.036430
38	1.023756	1.023968	1.023891	1.023833	1.023718	1.023577	1.023665	1.036159
39	1.023756	1.023968	1.023891	1.023833	1.023718	1.023582	1.023693	1.036194
40	1.012611	1.017632	1.015820	1.014451	1.011684	1.008762	1.012125	1.021888
41	1.012562	1.017610	1.015788	1.014412	1.011631	1.008803	1.012558	1.022472
42	1.011489	1.017035	1.015034	1.013521	1.010466	1.007209	1.010828	1.020245
43	1.010834	1.016694	1.014580	1.012981	1.009753	1.006323	1.010191	1.019443
44	1.009968	1.016252	1.013985	1.012271	1.008809	1.005153	1.009384	1.018424
45	1.009157	1.015845	1.013432	1.011608	1.007923	1.003963	1.008236	1.016940
46	1.005010	1.013982	1.010745	1.008298	1.003354	0.997698	1.002274	1.009103
47	1.002966	1.013065	1.009421	1.006667	1.001103	0.994611	0.999336	1.005240
48	1.002176	1.012712	1.008910	1.006037	1.000232	0.993415	0.998198	1.003744
49	1.001397	1.012402	1.008431	1.005430	0.999366	0.992225	0.997153	1.002350
50	1.000281	1.011904	1.007711	1.004541	0.998137	0.990562	0.995655	1.000383
51	1.000155	1.011843	1.007626	1.004438	0.997999	0.990358	0.995400	1.000047
52	1.000010	1.011771	1.007528	1.004320	0.997841	0.990125	0.995109	0.999666
53	0.999300	1.011419	1.007046	1.003741	0.997065	0.988985	0.993684	0.997795
54	0.998800	1.011149	1.006693	1.003326	0.996522	0.988209	0.992724	0.996549
55	1.005525	1.013973	1.010925	1.008621	1.003967	0.999069	1.004773	1.012572
56	1.005524	1.013972	1.010924	1.008620	1.003965	0.999067	1.004770	1.012568
57	1.002452	1.012400	1.008811	1.006098	1.000615	0.995266	1.003411	1.010974
58	1.002451	1.012399	1.008811	1.006098	1.000614	0.995267	1.003418	1.010982
59	1.024180	1.024291	1.024251	1.024221	1.024159	1.024093	1.024159	1.036739
60	1.023878	1.024081	1.024008	1.023952	1.023841	1.023692	1.023720	1.036201
61	1.023605	1.023920	1.023806	1.023720	1.023547	1.023337	1.023453	1.035876
62	1.023526	1.023873	1.023747	1.023652	1.023463	1.023235	1.023376	1.035782
63	1.023522	1.023871	1.023744	1.023649	1.023458	1.023229	1.023371	1.035775
64	1.022318	1.023164	1.022857	1.022626	1.022164	1.021614	1.021973	1.034042
65	1.021840	1.022876	1.022500	1.022217	1.021651	1.020987	1.021456	1.033407
66	1.021777	1.022838	1.022453	1.022163	1.021583	1.020904	1.021388	1.033324
67	1.021763	1.022830	1.022442	1.022151	1.021568	1.020885	1.021372	1.033305
68	1.021597	1.022729	1.022318	1.022009	1.021391	1.020667	1.021189	1.033080
69	1.021596	1.022729	1.022318	1.022009	1.021390	1.020667	1.021189	1.033080
Node	**8:00**	**9:00**	**10:00**	**11:00**	**12:00**	**13:00**	**14:00**	**15:00**
1	1.050000	1.050000	1.050000	1.050000	1.050000	1.050000	1.050000	1.050000
2	1.036852	1.036862	1.024315	1.024397	1.024343	1.036919	1.036954	1.036933
3	1.036666	1.036687	1.024240	1.024404	1.024297	1.036802	1.036871	1.036829
4	1.036568	1.036587	1.024155	1.024335	1.024219	1.036715	1.036782	1.036732
5	1.035581	1.035604	1.023444	1.023862	1.023602	1.035922	1.036024	1.035891
6	1.026556	1.026987	1.018842	1.022538	1.020125	1.029691	1.031071	1.030044
7	1.017936	1.018836	1.014742	1.021711	1.017119	1.023889	1.026680	1.024804
8	1.015950	1.016969	1.013840	1.021585	1.016473	1.022574	1.025717	1.023645
9	1.014895	1.015962	1.013308	1.021438	1.016071	1.021848	1.025143	1.022966

Table A1. *Cont.*

Node	8:00	9:00	10:00	11:00	12:00	13:00	14:00	15:00
10	1.005309	1.007076	1.009466	1.021557	1.013432	1.015780	1.021017	1.017874
11	1.003237	1.005109	1.008436	1.021274	1.012635	1.014365	1.019903	1.016555
12	0.998882	1.001331	1.007551	1.022525	1.012277	1.012055	1.019013	1.015247
13	0.993550	0.996536	1.005796	1.023012	1.011054	1.008889	1.017144	1.012866
14	0.988730	0.992296	1.004516	1.023879	1.010248	1.006183	1.015807	1.011078
15	0.984445	0.988633	1.003727	1.025137	1.009872	1.003955	1.015023	1.009905
16	0.983650	0.987954	1.003584	1.025374	1.009804	1.003543	1.014880	1.009690
17	0.981622	0.985997	1.002395	1.024774	1.008762	1.002066	1.013580	1.008200
18	0.981599	0.985975	1.002382	1.024768	1.008751	1.002049	1.013566	1.008184
19	0.980337	0.984799	1.001764	1.024554	1.008208	1.001192	1.012898	1.007405
20	0.979525	0.984043	1.001367	1.024417	1.007858	1.000642	1.012469	1.006904
21	0.978214	0.982823	1.000729	1.024199	1.007297	0.999754	1.011779	1.006099
22	0.978187	0.982801	1.000725	1.024207	1.007293	0.999740	1.011775	1.006093
23	0.978122	0.982803	1.000877	1.024435	1.007422	0.999790	1.011953	1.006275
24	0.977979	0.982808	1.001208	1.024932	1.007703	0.999898	1.012341	1.006673
25	0.978346	0.983528	1.002480	1.026416	1.008795	1.000707	1.013799	1.008226
26	0.978496	0.983825	1.003004	1.027028	1.009245	1.001040	1.014401	1.008867
27	0.978770	0.984190	1.003453	1.027482	1.009631	1.001387	1.014911	1.009420
28	1.036616	1.036636	1.024199	1.024374	1.024261	1.036759	1.036826	1.036780
29	1.036007	1.036011	1.023704	1.024009	1.023829	1.036237	1.036285	1.036188
30	1.033813	1.033828	1.022404	1.023494	1.022845	1.034629	1.034823	1.034476
31	1.033426	1.033443	1.022174	1.023404	1.022671	1.034346	1.034564	1.034174
32	1.031490	1.031516	1.021027	1.022950	1.021803	1.032927	1.033274	1.032664
33	1.027995	1.028109	1.019232	1.022549	1.020543	1.030506	1.031255	1.030249
34	1.025106	1.025629	1.019144	1.024363	1.021075	1.029215	1.031132	1.029787
35	1.021760	1.022100	1.016337	1.022310	1.018644	1.026344	1.027989	1.026271
36	1.036555	1.036574	1.024145	1.024326	1.024209	1.036705	1.036770	1.036720
37	1.036249	1.036263	1.023878	1.024115	1.023966	1.036436	1.036495	1.036419
38	1.035904	1.035916	1.023625	1.023977	1.023757	1.036177	1.036240	1.036113
39	1.035947	1.035964	1.023677	1.024036	1.023808	1.036228	1.036303	1.036174
40	1.016059	1.017113	1.014043	1.021822	1.016675	1.022726	1.025946	1.023885
41	1.016746	1.017942	1.015053	1.022911	1.017660	1.023540	1.027078	1.025086
42	1.013766	1.014893	1.012816	1.021415	1.015748	1.021114	1.024601	1.022305
43	1.012606	1.013809	1.012372	1.021483	1.015484	1.020391	1.024116	1.021697
44	1.011112	1.012429	1.011866	1.021670	1.015217	1.019494	1.023562	1.020982
45	1.009065	1.010379	1.010548	1.020985	1.014161	1.017941	1.022095	1.019299
46	0.998083	0.999397	1.003722	1.017745	1.008803	1.009754	1.014452	1.010444
47	0.992670	0.993984	1.000358	1.016151	1.006165	1.005719	1.010686	1.006080
48	0.990572	0.991887	0.999056	1.015537	1.005144	1.004157	1.009228	1.004390
49	0.988562	0.989908	0.997960	1.015183	1.004340	1.002741	1.007991	1.002923
50	0.985774	0.987154	0.996359	1.014555	1.003126	1.000731	1.006193	1.000819
51	0.985327	0.986683	0.995987	1.014281	1.002803	1.000349	1.005778	1.000355
52	0.984818	0.986149	0.995564	1.013970	1.002436	0.999914	1.005306	0.999828
53	0.982329	0.983532	0.993491	1.012444	1.000635	0.997786	1.002996	0.997247
54	0.980684	0.981805	0.992115	1.011420	0.999434	0.996374	1.001468	0.995544
55	1.002783	1.004631	1.008059	1.021000	1.012309	1.013978	1.019481	1.016082
56	1.002778	1.004625	1.008055	1.020997	1.012305	1.013973	1.019476	1.016076
57	0.999954	1.002702	1.009405	1.024638	1.014119	1.013469	1.021099	1.017444
58	0.999964	1.002714	1.009420	1.024653	1.014133	1.013481	1.021115	1.017462
59	1.036610	1.036629	1.024192	1.024368	1.024254	1.036753	1.036819	1.036772
60	1.035937	1.035933	1.023624	1.023942	1.023751	1.036176	1.036211	1.036095
61	1.035491	1.035512	1.023416	1.023922	1.023608	1.035881	1.035995	1.035829
62	1.035362	1.035390	1.023356	1.023917	1.023567	1.035796	1.035932	1.035753

Table A1. *Cont.*

Node	8:00	9:00	10:00	11:00	12:00	13:00	14:00	15:00
63	1.035354	1.035381	1.023351	1.023914	1.023562	1.035790	1.035926	1.035746
64	1.033029	1.033100	1.021959	1.023331	1.022474	1.034086	1.034436	1.034005
65	1.032177	1.032275	1.021483	1.023170	1.022113	1.033480	1.033932	1.033410
66	1.032064	1.032166	1.021421	1.023149	1.022065	1.033400	1.033866	1.033331
67	1.032039	1.032141	1.021406	1.023144	1.022054	1.033382	1.033850	1.033313
68	1.031739	1.031850	1.021233	1.023080	1.021921	1.033166	1.033668	1.033098
69	1.031738	1.031849	1.021233	1.023080	1.021921	1.033166	1.033668	1.033098
Node	**16:00**	**17:00**	**18:00**	**19:00**	**20:00**	**21:00**	**22:00**	**23:00**
1	1.050000	1.050000	1.050000	1.050000	1.050000	1.050000	1.050000	1.050000
2	1.036920	1.036903	1.036864	1.036860	1.036840	1.036869	1.024259	1.024297
3	1.036804	1.036769	1.036690	1.036683	1.036644	1.036702	1.024128	1.024204
4	1.036712	1.036678	1.036604	1.036604	1.036566	1.036630	1.024063	1.024148
5	1.035887	1.035829	1.035720	1.035768	1.035706	1.035861	1.023406	1.023609
6	1.029617	1.028911	1.027327	1.027313	1.026493	1.027860	1.016909	1.018692
7	1.023840	1.022431	1.019198	1.018994	1.017344	1.019911	1.010451	1.013801
8	1.022540	1.020957	1.017310	1.017046	1.015190	1.018040	1.008931	1.012651
9	1.021810	1.020150	1.016331	1.016061	1.014117	1.017110	1.008178	1.012083
10	1.015870	1.013280	1.007186	1.006514	1.003433	1.007920	1.000850	1.006702
11	1.014445	1.011708	1.005280	1.004602	1.001348	1.006124	0.999413	1.005641
12	1.012369	1.008981	1.000826	0.999586	0.995489	1.001098	0.995422	1.002728
13	1.009334	1.005354	0.995684	0.994093	0.989237	0.995767	0.991236	0.999731
14	1.006813	1.002215	0.990926	0.988880	0.983224	0.990638	0.987205	0.996840
15	1.004824	0.999582	0.986566	0.983959	0.977461	0.985719	0.983336	0.994061
16	1.004457	0.999094	0.985756	0.983045	0.976390	0.984805	0.982617	0.993544
17	1.002926	0.997482	0.983994	0.981380	0.974638	0.983311	0.981442	0.992702
18	1.002910	0.997464	0.983974	0.981360	0.974617	0.983293	0.981428	0.992692
19	1.002045	0.996518	0.982836	0.980228	0.973384	0.982242	0.980605	0.992104
20	1.001490	0.995909	0.982105	0.979499	0.972591	0.981567	0.980076	0.991726
21	1.000594	0.994928	0.980923	0.978322	0.971308	0.980475	0.979219	0.991114
22	1.000583	0.994912	0.980896	0.978291	0.971272	0.980444	0.979196	0.991098
23	1.000670	0.994949	0.980775	0.978088	0.970994	0.980208	0.979014	0.990971
24	1.000862	0.995029	0.980512	0.977645	0.970387	0.979695	0.978617	0.990694
25	1.001902	0.995814	0.980473	0.977113	0.969467	0.978920	0.978022	0.990287
26	1.002331	0.996138	0.980457	0.976893	0.969088	0.978600	0.977777	0.990118
27	1.002746	0.996490	0.980595	0.976886	0.968981	0.978510	0.977708	0.990071
28	1.036758	1.036724	1.036649	1.036647	1.036609	1.036671	1.024102	1.024183
29	1.036207	1.036169	1.036137	1.036201	1.036179	1.036288	1.023779	1.023924
30	1.034527	1.034396	1.034251	1.034465	1.034374	1.034757	1.022597	1.023108
31	1.034231	1.034082	1.033918	1.034159	1.034056	1.034487	1.022388	1.022964
32	1.032749	1.032517	1.032254	1.032627	1.032464	1.033137	1.021345	1.022245
33	1.030271	1.029810	1.029149	1.029645	1.029274	1.030425	1.019243	1.020784
34	1.029216	1.028172	1.026122	1.026169	1.025144	1.026921	1.016536	1.018914
35	1.026068	1.025113	1.023519	1.024121	1.023278	1.025335	1.015306	1.018058
36	1.036701	1.036667	1.036593	1.036593	1.036556	1.036620	1.024055	1.024140
37	1.036416	1.036385	1.036317	1.036336	1.036301	1.036383	1.023839	1.023948
38	1.036125	1.036096	1.036005	1.036031	1.035987	1.036104	1.023601	1.023756
39	1.036177	1.036145	1.036031	1.036040	1.035987	1.036104	1.023601	1.023756
40	1.022723	1.021106	1.017353	1.017022	1.015119	1.017978	1.008880	1.012611
41	1.023677	1.021924	1.017737	1.017114	1.015018	1.017892	1.008812	1.012562
42	1.021079	1.019319	1.015277	1.014990	1.012937	1.016094	1.007368	1.011489
43	1.020372	1.018491	1.014169	1.013835	1.011646	1.014983	1.006479	1.010834
44	1.019507	1.017453	1.012723	1.012308	1.009922	1.013500	1.005299	1.009968
45	1.017873	1.015757	1.010974	1.010716	1.008291	1.012100	1.004186	1.009157
46	1.009258	1.006767	1.001613	1.002194	0.999517	1.004627	0.998342	1.005010
47	1.005012	1.002337	0.996999	0.997994	0.995193	1.000944	0.995462	1.002966
48	1.003367	1.000621	0.995211	0.996366	0.993517	0.999516	0.994346	1.002176
49	1.001895	0.999043	0.993465	0.994728	0.991787	0.998053	0.993219	1.001397

Table A1. *Cont.*

Node	16:00	17:00	18:00	19:00	20:00	21:00	22:00	23:00
50	0.999801	0.996818	0.991047	0.992472	0.989420	0.996038	0.991644	1.000281
51	0.999383	0.996410	0.990696	0.992192	0.989163	0.995818	0.991470	1.000155
52	0.998909	0.995948	0.990298	0.991873	0.988870	0.995567	0.991271	1.000010
53	0.996584	0.993681	0.988344	0.990313	0.987436	0.994336	0.990295	0.999300
54	0.995046	0.992180	0.987044	0.989267	0.986470	0.993502	0.989624	0.998800
55	1.014021	1.011295	1.004927	1.004324	1.001094	1.005909	0.999246	1.005525
56	1.014016	1.011290	1.004923	1.004320	1.001091	1.005906	0.999244	1.005524
57	1.014062	1.010381	1.001305	0.999474	0.994961	1.000641	0.995052	1.002452
58	1.014076	1.010393	1.001310	0.999475	0.994960	1.000639	0.995051	1.002451
59	1.036751	1.036717	1.036643	1.036642	1.036605	1.036666	1.024098	1.024180
60	1.036126	1.036104	1.036075	1.036145	1.036125	1.036237	1.023730	1.023878
61	1.035831	1.035772	1.035645	1.035697	1.035633	1.035805	1.023374	1.023605
62	1.035746	1.035676	1.035521	1.035568	1.035490	1.035680	1.023272	1.023526
63	1.035739	1.035669	1.035514	1.035561	1.035483	1.035674	1.023267	1.023522
64	1.033974	1.033795	1.033400	1.033503	1.033307	1.033767	1.021700	1.022318
65	1.033353	1.033124	1.032607	1.032711	1.032457	1.033021	1.021083	1.021840
66	1.033271	1.033035	1.032502	1.032606	1.032345	1.032922	1.021002	1.021777
67	1.033252	1.033015	1.032479	1.032583	1.032320	1.032901	1.020984	1.021763
68	1.033030	1.032777	1.032202	1.032308	1.032027	1.032643	1.020770	1.021597
69	1.033030	1.032776	1.032201	1.032307	1.032026	1.032642	1.020769	1.021596

Table A2. Voltage results obtained by S1 of Case 1 (p.u.).

Node	0:00	1:00	2:00	3:00	4:00	5:00	6:00	7:00
1	1.050000	1.050000	1.050000	1.050000	1.050000	1.050000	1.050000	1.050000
2	1.024297	1.024349	1.024331	1.024316	1.024288	1.024258	1.024293	1.036912
3	1.024204	1.024308	1.024271	1.024242	1.024185	1.024126	1.024197	1.036786
4	1.024148	1.024262	1.024221	1.024190	1.024127	1.024058	1.024126	1.036706
5	1.023609	1.023882	1.023783	1.023709	1.023558	1.023377	1.023483	1.035945
6	1.018692	1.021093	1.020227	1.019572	1.018249	1.016822	1.018289	1.029551
7	1.013801	1.018310	1.016683	1.015453	1.012969	1.010355	1.013343	1.023488
8	1.012651	1.017657	1.015851	1.014486	1.011728	1.008840	1.012208	1.022100
9	1.012083	1.017339	1.015443	1.014009	1.011114	1.008079	1.011607	1.021357
10	1.006702	1.014576	1.011735	1.009588	1.005249	1.000800	1.006416	1.014868
11	1.005641	1.014019	1.010997	1.008712	1.004095	0.999346	1.005275	1.013435
12	1.002728	1.012552	1.009009	1.006330	1.000915	0.995514	1.003044	1.010688
13	0.999731	1.011142	1.007028	1.003916	0.997623	0.991382	1.000267	1.007153
14	0.996840	1.009774	1.005111	1.001584	0.994450	0.987447	0.997780	1.004008
15	0.994061	1.008450	1.003264	0.999339	0.991401	0.983717	0.995594	1.001267
16	0.993544	1.008204	1.002920	0.998923	0.990834	0.983024	0.995188	1.000758
17	0.992702	1.007805	1.002362	0.998243	0.989909	0.981790	0.994086	0.999330
18	0.992692	1.007800	1.002355	0.998235	0.989898	0.981775	0.994074	0.999314
19	0.992104	1.007527	1.001968	0.997762	0.989252	0.980933	0.993404	0.998449
20	0.991726	1.007351	1.001720	0.997459	0.988836	0.980392	0.992973	0.997893
21	0.991114	1.007067	1.001318	0.996968	0.988165	0.979517	0.992279	0.996996
22	0.991098	1.007061	1.001308	0.996955	0.988147	0.979495	0.992266	0.996980
23	0.990971	1.007007	1.001228	0.996855	0.988006	0.979339	0.992255	0.996970
24	0.990694	1.006891	1.001054	0.996637	0.987699	0.979000	0.992229	0.996950

Table A2. *Cont.*

Node	0:00	1:00	2:00	3:00	4:00	5:00	6:00	7:00
25	0.990287	1.006732	1.000806	0.996321	0.987245	0.978576	0.992560	0.997412
26	0.990118	1.006666	1.000703	0.996190	0.987058	0.978401	0.992696	0.997602
27	0.990071	1.006648	1.000674	0.996154	0.987005	0.978385	0.992876	0.997848
28	1.024183	1.024294	1.024254	1.024224	1.024163	1.024097	1.024163	1.036745
29	1.023924	1.024122	1.024051	1.023997	1.023888	1.023739	1.023750	1.036234
30	1.023108	1.023808	1.023554	1.023363	1.022981	1.022473	1.022566	1.034660
31	1.022964	1.023752	1.023466	1.023252	1.022821	1.022250	1.022357	1.034382
32	1.022245	1.023475	1.023028	1.022693	1.022020	1.021133	1.021313	1.032994
33	1.020784	1.022891	1.022126	1.021552	1.020400	1.018937	1.019436	1.030514
34	1.018914	1.022164	1.020984	1.020098	1.018320	1.016331	1.018008	1.028642
35	1.018058	1.021818	1.020454	1.019428	1.017371	1.014868	1.016129	1.026138
36	1.024140	1.024256	1.024214	1.024182	1.024119	1.024049	1.024117	1.036695
37	1.023948	1.024097	1.024043	1.024002	1.023921	1.023824	1.023884	1.036434
38	1.023756	1.023968	1.023891	1.023833	1.023718	1.023579	1.023655	1.036159
39	1.023756	1.023968	1.023891	1.023833	1.023718	1.023585	1.023680	1.036193
40	1.012611	1.017632	1.015820	1.014451	1.011684	1.008813	1.012276	1.022198
41	1.012562	1.017610	1.015788	1.014412	1.011631	1.008854	1.012707	1.022784
42	1.011489	1.017035	1.015034	1.013521	1.010466	1.007265	1.010993	1.020583
43	1.010834	1.016694	1.014580	1.012981	1.009753	1.006382	1.010364	1.019796
44	1.009968	1.016252	1.013985	1.012271	1.008809	1.005216	1.009566	1.018797
45	1.009157	1.015845	1.013432	1.011608	1.007923	1.004029	1.008430	1.017331
46	1.005010	1.013982	1.010745	1.008298	1.003354	0.997778	1.002510	1.009571
47	1.002966	1.013065	1.009421	1.006667	1.001103	0.994698	0.999593	1.005746
48	1.002176	1.012712	1.008910	1.006037	1.000232	0.993505	0.998464	1.004264
49	1.001397	1.012402	1.008431	1.005430	0.999366	0.992318	0.997428	1.002887
50	1.000281	1.011904	1.007711	1.004541	0.998137	0.990660	0.995950	1.000953
51	1.000155	1.011843	1.007626	1.004438	0.997999	0.990457	0.995695	1.000617
52	1.000010	1.011771	1.007528	1.004320	0.997841	0.990224	0.995404	1.000236
53	0.999300	1.011419	1.007046	1.003741	0.997065	0.989084	0.993979	0.998366
54	0.998800	1.011149	1.006693	1.003326	0.996522	0.988308	0.993020	0.997121
55	1.005525	1.013973	1.010925	1.008621	1.003967	0.999148	1.005022	1.013097
56	1.005524	1.013972	1.010924	1.008620	1.003965	0.999145	1.005019	1.013094
57	1.002452	1.012400	1.008811	1.006098	1.000615	0.995380	1.003794	1.011736
58	1.002451	1.012399	1.008811	1.006098	1.000614	0.995381	1.003801	1.011745
59	1.024180	1.024291	1.024251	1.024221	1.024159	1.024093	1.024160	1.036741
60	1.023878	1.024081	1.024008	1.023952	1.023841	1.023693	1.023716	1.036202
61	1.023605	1.023920	1.023806	1.023720	1.023547	1.023339	1.023446	1.035877
62	1.023526	1.023873	1.023747	1.023652	1.023463	1.023236	1.023368	1.035783
63	1.023522	1.023871	1.023744	1.023649	1.023458	1.023231	1.023363	1.035777
64	1.022318	1.023164	1.022857	1.022626	1.022164	1.021618	1.021956	1.034045
65	1.021840	1.022876	1.022500	1.022217	1.021651	1.020992	1.021434	1.033411
66	1.021777	1.022838	1.022453	1.022163	1.021583	1.020909	1.021365	1.033327
67	1.021763	1.022830	1.022442	1.022151	1.021568	1.020890	1.021349	1.033308
68	1.021597	1.022729	1.022318	1.022009	1.021391	1.020673	1.021165	1.033084
69	1.021596	1.022729	1.022318	1.022009	1.021390	1.020672	1.021165	1.033084
Node	**8:00**	**9:00**	**10:00**	**11:00**	**12:00**	**13:00**	**14:00**	**15:00**
1	1.050000	1.050000	1.050000	1.050000	1.050000	1.050000	1.050000	1.050000
2	1.036853	1.036857	1.024321	1.024400	1.024349	1.036919	1.036954	1.036930
3	1.036670	1.036678	1.024252	1.024409	1.024309	1.036801	1.036870	1.036822
4	1.036574	1.036579	1.024170	1.024343	1.024234	1.036716	1.036784	1.036729
5	1.035607	1.035603	1.023495	1.023900	1.023654	1.035937	1.036050	1.035910
6	1.026758	1.026885	1.019265	1.022851	1.020597	1.029792	1.031233	1.030090
7	1.018320	1.018626	1.015551	1.022307	1.018026	1.024077	1.026980	1.024871
8	1.016378	1.016733	1.014742	1.022249	1.017485	1.022783	1.026049	1.023716
9	1.015346	1.015716	1.014256	1.022138	1.017137	1.022070	1.025493	1.023042
10	1.005990	1.006643	1.010907	1.022712	1.015176	1.016130	1.021522	1.017915
11	1.003970	1.004652	1.009979	1.022536	1.014527	1.014751	1.020450	1.016604

Table A2. *Cont.*

Node	8:00	9:00	10:00	11:00	12:00	13:00	14:00	15:00
12	0.999797	1.000766	1.009458	1.024176	1.014712	1.012564	1.019700	1.015300
13	0.994537	0.995704	1.007921	1.024999	1.014003	1.009410	1.017803	1.012717
14	0.989790	0.991191	1.006862	1.026209	1.013718	1.006717	1.016438	1.010723
15	0.985580	0.987252	1.006299	1.027817	1.013874	1.004503	1.015626	1.009339
16	0.984798	0.986521	1.006197	1.028120	1.013905	1.004094	1.015478	1.009085
17	0.982791	0.984497	1.005062	1.027648	1.013036	1.002630	1.014177	1.007544
18	0.982768	0.984474	1.005050	1.027644	1.013026	1.002614	1.014163	1.007528
19	0.981523	0.983240	1.004478	1.027542	1.012632	1.001769	1.013494	1.006704
20	0.980722	0.982447	1.004110	1.027477	1.012379	1.001227	1.013065	1.006175
21	0.979429	0.981166	1.003520	1.027375	1.011973	1.000351	1.012374	1.005324
22	0.979403	0.981141	1.003518	1.027388	1.011976	1.000338	1.012370	1.005316
23	0.979345	0.981116	1.003691	1.027669	1.012176	1.000394	1.012547	1.005477
24	0.979219	0.981062	1.004067	1.028283	1.012611	1.000514	1.012934	1.005829
25	0.979621	0.981655	1.005437	1.030017	1.014036	1.001350	1.014390	1.007284
26	0.979786	0.981899	1.006002	1.030733	1.014623	1.001694	1.014990	1.007884
27	0.980068	0.982235	1.006473	1.031244	1.015084	1.002046	1.015499	1.008415
28	1.036618	1.036623	1.024207	1.024375	1.024269	1.036756	1.036822	1.036769
29	1.035968	1.035947	1.023659	1.023955	1.023783	1.036190	1.036222	1.036109
30	1.033748	1.033689	1.022341	1.023393	1.022773	1.034541	1.034701	1.034311
31	1.033357	1.033291	1.022109	1.023295	1.022594	1.034250	1.034433	1.033994
32	1.031398	1.031298	1.020946	1.022800	1.021703	1.032795	1.033091	1.032408
33	1.027847	1.027733	1.019112	1.022300	1.020387	1.030284	1.030948	1.029812
34	1.024848	1.024936	1.018952	1.023917	1.020810	1.028816	1.030580	1.028987
35	1.021501	1.021404	1.016145	1.021864	1.018379	1.025944	1.027436	1.025469
36	1.036561	1.036566	1.024160	1.024334	1.024225	1.036705	1.036773	1.036717
37	1.036253	1.036252	1.023897	1.024120	1.023984	1.036431	1.036495	1.036420
38	1.035901	1.035896	1.023659	1.023976	1.023783	1.036150	1.036233	1.036124
39	1.035941	1.035942	1.023714	1.024033	1.023836	1.036195	1.036294	1.036188
40	1.016489	1.016870	1.014952	1.022485	1.017693	1.022932	1.026276	1.023951
41	1.017181	1.017672	1.015986	1.023574	1.018695	1.023739	1.027400	1.025130
42	1.014236	1.014628	1.013804	1.022132	1.016846	1.021340	1.024962	1.022374
43	1.013097	1.013524	1.013406	1.022220	1.016620	1.020620	1.024489	1.021758
44	1.011634	1.012114	1.012964	1.022433	1.016405	1.019729	1.023951	1.021032
45	1.009613	1.010056	1.011690	1.021776	1.015386	1.018190	1.022507	1.019354
46	0.998746	0.998995	1.005075	1.018643	1.010203	1.010047	1.014940	1.010472
47	0.993390	0.993543	1.001815	1.017101	1.007650	1.006034	1.011211	1.006095
48	0.991314	0.991430	1.000553	1.016506	1.006663	1.004479	1.009767	1.004399
49	0.989330	0.989431	0.999506	1.016176	1.005899	1.003072	1.008545	1.002923
50	0.986589	0.986664	0.997982	1.015596	1.004751	1.001087	1.006788	1.000828
51	0.986142	0.986193	0.997611	1.015323	1.004429	1.000705	1.006373	1.000363
52	0.985634	0.985658	0.997188	1.015012	1.004062	1.000270	1.005902	0.999837
53	0.983147	0.983040	0.995118	1.013487	1.002263	0.998142	1.003593	0.997255
54	0.981504	0.981312	0.993745	1.012465	1.001064	0.996731	1.002066	0.995552
55	1.003516	1.004174	1.009602	1.022263	1.014202	1.014364	1.020028	1.016132
56	1.003511	1.004168	1.009598	1.022260	1.014198	1.014359	1.020023	1.016126
57	1.001002	1.002215	1.011530	1.026449	1.016748	1.014093	1.021947	1.017639
58	1.001013	1.002228	1.011546	1.026466	1.016763	1.014106	1.021964	1.017657
59	1.036613	1.036619	1.024204	1.024373	1.024266	1.036752	1.036818	1.036765
60	1.035937	1.035919	1.023642	1.023944	1.023767	1.036165	1.036207	1.036094
61	1.035492	1.035485	1.023448	1.023922	1.023633	1.035862	1.035985	1.035823
62	1.035363	1.035359	1.023392	1.023915	1.023595	1.035774	1.035922	1.035744
63	1.035355	1.035351	1.023386	1.023912	1.023590	1.035767	1.035916	1.035737
64	1.033030	1.033025	1.022042	1.023322	1.022535	1.034033	1.034408	1.033979
65	1.032179	1.032180	1.021587	1.023158	1.022187	1.033413	1.033897	1.033377
66	1.032066	1.032069	1.021527	1.023137	1.022141	1.033331	1.033830	1.033297
67	1.032041	1.032044	1.021513	1.023131	1.022131	1.033313	1.033814	1.033279

Table A2. *Cont.*

Node	8:00	9:00	10:00	11:00	12:00	13:00	14:00	15:00
68	1.031741	1.031745	1.021347	1.023065	1.022002	1.033092	1.033628	1.033061
69	1.031740	1.031745	1.021347	1.023066	1.022003	1.033092	1.033629	1.033062
Node	**16:00**	**17:00**	**18:00**	**19:00**	**20:00**	**21:00**	**22:00**	**23:00**
1	1.050000	1.050000	1.050000	1.050000	1.050000	1.050000	1.050000	1.050000
2	1.036922	1.036900	1.036866	1.036861	1.036840	1.036869	1.024259	1.024297
3	1.036808	1.036764	1.036694	1.036686	1.036644	1.036702	1.024128	1.024204
4	1.036719	1.036675	1.036609	1.036607	1.036566	1.036630	1.024063	1.024148
5	1.035920	1.035837	1.035738	1.035778	1.035706	1.035861	1.023406	1.023609
6	1.029867	1.028913	1.027475	1.027397	1.026493	1.027860	1.016909	1.018692
7	1.024314	1.022425	1.019480	1.019156	1.017344	1.019911	1.010451	1.013801
8	1.023067	1.020948	1.017625	1.017227	1.015190	1.018040	1.008931	1.012651
9	1.022365	1.020143	1.016662	1.016251	1.014117	1.017110	1.008178	1.012083
10	1.016708	1.013247	1.007682	1.006802	1.003433	1.007920	1.000850	1.006702
11	1.015347	1.011683	1.005810	1.004910	1.001348	1.006124	0.999413	1.005641
12	1.013495	1.008970	1.001479	0.999966	0.995489	1.001098	0.995422	1.002728
13	1.010545	1.005234	0.996383	0.994518	0.989237	0.995767	0.991236	0.999731
14	1.008109	1.001984	0.991671	0.989350	0.983224	0.990638	0.987205	0.996840
15	1.006209	0.999238	0.987358	0.984475	0.977461	0.985719	0.983336	0.994061
16	1.005858	0.998730	0.986557	0.983569	0.976390	0.984805	0.982617	0.993544
17	1.004353	0.997100	0.984803	0.981914	0.974638	0.983311	0.981442	0.992702
18	1.004336	0.997082	0.984783	0.981894	0.974617	0.983293	0.981428	0.992692
19	1.003494	0.996120	0.983651	0.980770	0.973384	0.982242	0.980605	0.992104
20	1.002952	0.995502	0.982923	0.980047	0.972591	0.981567	0.980076	0.991726
21	1.002080	0.994505	0.981748	0.978878	0.971308	0.980475	0.979219	0.991114
22	1.002069	0.994488	0.981721	0.978848	0.971272	0.980444	0.979196	0.991098
23	1.002167	0.994518	0.981602	0.978649	0.970994	0.980208	0.979014	0.990971
24	1.002380	0.994582	0.981345	0.978214	0.970387	0.979695	0.978617	0.990694
25	1.003466	0.995333	0.981318	0.977700	0.969467	0.978920	0.978022	0.990287
26	1.003914	0.995643	0.981306	0.977487	0.969088	0.978600	0.977777	0.990118
27	1.004340	0.995987	0.981447	0.977484	0.968981	0.978510	0.977708	0.990071
28	1.036759	1.036715	1.036651	1.036649	1.036609	1.036671	1.024102	1.024183
29	1.036153	1.036118	1.036116	1.036195	1.036179	1.036288	1.023779	1.023924
30	1.034432	1.034287	1.034220	1.034459	1.034374	1.034757	1.022597	1.023108
31	1.034128	1.033964	1.033886	1.034152	1.034056	1.034487	1.022388	1.022964
32	1.032610	1.032348	1.032213	1.032620	1.032464	1.033137	1.021345	1.022245
33	1.030045	1.029520	1.029088	1.029635	1.029274	1.030425	1.019243	1.020784
34	1.028819	1.027638	1.026021	1.026157	1.025144	1.026921	1.016536	1.018914
35	1.025669	1.024578	1.023418	1.024108	1.023278	1.025335	1.015306	1.018058
36	1.036708	1.036663	1.036598	1.036597	1.036556	1.036620	1.024055	1.024140
37	1.036423	1.036377	1.036321	1.036340	1.036301	1.036383	1.023839	1.023948
38	1.036135	1.036074	1.036005	1.036039	1.035987	1.036104	1.023601	1.023756
39	1.036188	1.036119	1.036030	1.036048	1.035987	1.036104	1.023601	1.023756
40	1.023251	1.021092	1.017670	1.017204	1.015119	1.017978	1.008880	1.012611
41	1.024211	1.021891	1.018062	1.017302	1.015018	1.017892	1.008812	1.012562
42	1.021654	1.019304	1.015624	1.015188	1.012937	1.016094	1.007368	1.011489
43	1.020970	1.018467	1.014533	1.014044	1.011646	1.014983	1.006479	1.010834
44	1.020139	1.017418	1.013114	1.012530	1.009922	1.013500	1.005299	1.009968
45	1.018533	1.015725	1.011383	1.010947	1.008291	1.012100	1.004186	1.009157
46	1.010036	1.006719	1.002113	1.002471	0.999517	1.004627	0.998342	1.005010
47	1.005848	1.002281	0.997544	0.998293	0.995193	1.000944	0.995462	1.002966
48	1.004225	1.000561	0.995773	0.996673	0.993517	0.999516	0.994346	1.002176
49	1.002779	0.998977	0.994048	0.995046	0.991787	0.998053	0.993219	1.001397
50	1.000735	0.996759	0.991664	0.992806	0.989420	0.996038	0.991644	1.000281
51	1.000318	0.996352	0.991313	0.992526	0.989163	0.995818	0.991470	1.000155
52	0.999844	0.995889	0.990915	0.992208	0.988870	0.995567	0.991271	1.000010
53	0.997521	0.993622	0.988962	0.990648	0.987436	0.994336	0.990295	0.999300
54	0.995985	0.992121	0.987664	0.989602	0.986470	0.993502	0.989624	0.998800
55	1.014923	1.011270	1.005457	1.004632	1.001094	1.005909	0.999246	1.005525

Table A2. *Cont.*

Node	16:00	17:00	18:00	19:00	20:00	21:00	22:00	23:00
56	1.014918	1.011265	1.005453	1.004629	1.001091	1.005906	0.999244	1.005524
57	1.015356	1.010461	1.002051	0.999896	0.994961	1.000641	0.995052	1.002452
58	1.015371	1.010473	1.002057	0.999897	0.994960	1.000639	0.995051	1.002451
59	1.036755	1.036712	1.036647	1.036645	1.036605	1.036666	1.024098	1.024180
60	1.036132	1.036092	1.036077	1.036149	1.036125	1.036237	1.023730	1.023878
61	1.035839	1.035748	1.035649	1.035704	1.035633	1.035805	1.023374	1.023605
62	1.035755	1.035649	1.035526	1.035576	1.035490	1.035680	1.023272	1.023526
63	1.035748	1.035642	1.035519	1.035569	1.035483	1.035674	1.023267	1.023522
64	1.033993	1.033728	1.033412	1.033522	1.033307	1.033767	1.021700	1.022318
65	1.033377	1.033040	1.032622	1.032734	1.032457	1.033021	1.021083	1.021840
66	1.033295	1.032949	1.032518	1.032630	1.032345	1.032922	1.021002	1.021777
67	1.033277	1.032929	1.032495	1.032607	1.032320	1.032901	1.020984	1.021763
68	1.033056	1.032684	1.032218	1.032334	1.032027	1.032643	1.020770	1.021597
69	1.033056	1.032684	1.032217	1.032333	1.032026	1.032642	1.020769	1.021596

Table A3. Voltage results obtained by S2 of Case 1 (p.u.).

Node	0:00	1:00	2:00	3:00	4:00	5:00	6:00	7:00
1	1.050000	1.050000	1.050000	1.050000	1.050000	1.050000	1.050000	1.050000
2	1.024297	1.024349	1.024331	1.024316	1.024288	1.024258	1.024293	1.036913
3	1.024204	1.024308	1.024271	1.024242	1.024185	1.024126	1.024196	1.036788
4	1.024148	1.024262	1.024221	1.024190	1.024127	1.024057	1.024125	1.036711
5	1.023609	1.023882	1.023783	1.023709	1.023558	1.023373	1.023478	1.035970
6	1.018692	1.021093	1.020227	1.019572	1.018249	1.016795	1.018261	1.029687
7	1.013801	1.018310	1.016683	1.015453	1.012969	1.010304	1.013290	1.023740
8	1.012651	1.017657	1.015851	1.014486	1.011728	1.008783	1.012149	1.022379
9	1.012083	1.017339	1.015443	1.014009	1.011114	1.008020	1.011545	1.021649
10	1.006702	1.014576	1.011735	1.009588	1.005249	1.000716	1.006348	1.015232
11	1.005641	1.014019	1.010997	1.008712	1.004095	0.999258	1.005206	1.013813
12	1.002728	1.012552	1.009009	1.006330	1.000915	0.995410	1.002971	1.011108
13	0.999731	1.011142	1.007028	1.003916	0.997623	0.991263	1.000188	1.007631
14	0.996840	1.009774	1.005111	1.001584	0.994450	0.987311	0.997695	1.004542
15	0.994061	1.008450	1.003264	0.999339	0.991401	0.983564	0.995503	1.001856
16	0.993544	1.008204	1.002920	0.998923	0.990834	0.982868	0.995096	1.001358
17	0.992702	1.007805	1.002362	0.998243	0.989909	0.981631	0.993993	0.999940
18	0.992692	1.007800	1.002355	0.998235	0.989898	0.981616	0.993981	0.999924
19	0.992104	1.007527	1.001968	0.997762	0.989252	0.980772	0.993310	0.999068
20	0.991726	1.007351	1.001720	0.997459	0.988836	0.980229	0.992878	0.998517
21	0.991114	1.007067	1.001318	0.996968	0.988165	0.979351	0.992183	0.997629
22	0.991098	1.007061	1.001308	0.996955	0.988147	0.979329	0.992170	0.997613
23	0.990971	1.007007	1.001228	0.996855	0.988006	0.979172	0.992158	0.997608
24	0.990694	1.006891	1.001054	0.996637	0.987699	0.978830	0.992132	0.997596
25	0.990287	1.006732	1.000806	0.996321	0.987245	0.978401	0.992460	0.998076
26	0.990118	1.006666	1.000703	0.996190	0.987058	0.978224	0.992595	0.998274
27	0.990071	1.006648	1.000674	0.996154	0.987005	0.978206	0.992775	0.998524
28	1.024183	1.024294	1.024254	1.024224	1.024163	1.024096	1.024163	1.036748
29	1.023924	1.024122	1.024051	1.023997	1.023888	1.023736	1.023748	1.036253
30	1.023108	1.023808	1.023554	1.023363	1.022981	1.022467	1.022564	1.034689
31	1.022964	1.023752	1.023466	1.023252	1.022821	1.022244	1.022355	1.034413
32	1.022245	1.023475	1.023028	1.022693	1.022020	1.021124	1.021309	1.033033

Table A3. *Cont.*

Node	0:00	1:00	2:00	3:00	4:00	5:00	6:00	7:00
33	1.020784	1.022891	1.022126	1.021552	1.020400	1.018922	1.019430	1.030574
34	1.018914	1.022164	1.020984	1.020098	1.018320	1.016303	1.017998	1.028743
35	1.018058	1.021818	1.020454	1.019428	1.017371	1.014840	1.016118	1.026239
36	1.024140	1.024256	1.024214	1.024182	1.024119	1.024048	1.024116	1.036701
37	1.023948	1.024097	1.024043	1.024002	1.023921	1.023820	1.023882	1.036461
38	1.023756	1.023968	1.023891	1.023833	1.023718	1.023564	1.023650	1.036259
39	1.023756	1.023968	1.023891	1.023833	1.023718	1.023567	1.023674	1.036314
40	1.012611	1.017632	1.015820	1.014451	1.011684	1.008755	1.012216	1.022481
41	1.012562	1.017610	1.015788	1.014412	1.011631	1.008794	1.012647	1.023075
42	1.011489	1.017035	1.015034	1.013521	1.010466	1.007203	1.010922	1.020891
43	1.010834	1.016694	1.014580	1.012981	1.009753	1.006317	1.010282	1.020123
44	1.009968	1.016252	1.013985	1.012271	1.008809	1.005148	1.009470	1.019152
45	1.009157	1.015845	1.013432	1.011608	1.007923	1.003960	1.008320	1.017700
46	1.005010	1.013982	1.010745	1.008298	1.003354	0.997703	1.002349	1.009989
47	1.002966	1.013065	1.009421	1.006667	1.001103	0.994619	0.999406	1.006188
48	1.002176	1.012712	1.008910	1.006037	1.000232	0.993425	0.998267	1.004716
49	1.001397	1.012402	1.008431	1.005430	0.999366	0.992237	0.997220	1.003349
50	1.000281	1.011904	1.007711	1.004541	0.998137	0.990577	0.995718	1.001441
51	1.000155	1.011843	1.007626	1.004438	0.997999	0.990373	0.995463	1.001105
52	1.000010	1.011771	1.007528	1.004320	0.997841	0.990141	0.995172	1.000724
53	0.999300	1.011419	1.007046	1.003741	0.997065	0.989001	0.993747	0.998855
54	0.998800	1.011149	1.006693	1.003326	0.996522	0.988225	0.992787	0.997611
55	1.005525	1.013973	1.010925	1.008621	1.003967	0.999060	1.004953	1.013475
56	1.005524	1.013972	1.010924	1.008620	1.003965	0.999057	1.004950	1.013471
57	1.002452	1.012400	1.008811	1.006098	1.000615	0.995272	1.003722	1.012157
58	1.002451	1.012399	1.008811	1.006098	1.000614	0.995273	1.003729	1.012166
59	1.024180	1.024291	1.024251	1.024221	1.024159	1.024092	1.024159	1.036745
60	1.023878	1.024081	1.024008	1.023952	1.023841	1.023687	1.023714	1.036239
61	1.023605	1.023920	1.023806	1.023720	1.023547	1.023329	1.023443	1.035937
62	1.023526	1.023873	1.023747	1.023652	1.023463	1.023226	1.023365	1.035850
63	1.023522	1.023871	1.023744	1.023649	1.023458	1.023220	1.023359	1.035844
64	1.022318	1.023164	1.022857	1.022626	1.022164	1.021594	1.021947	1.034195
65	1.021840	1.022876	1.022500	1.022217	1.021651	1.020961	1.021423	1.033596
66	1.021777	1.022838	1.022453	1.022163	1.021583	1.020878	1.021354	1.033517
67	1.021763	1.022830	1.022442	1.022151	1.021568	1.020859	1.021338	1.033500
68	1.021597	1.022729	1.022318	1.022009	1.021391	1.020640	1.021153	1.033289
69	1.021596	1.022729	1.022318	1.022009	1.021390	1.020639	1.021153	1.033289
Node	**8:00**	**9:00**	**10:00**	**11:00**	**12:00**	**13:00**	**14:00**	**15:00**
1	1.050000	1.050000	1.050000	1.050000	1.050000	1.050000	1.050000	1.050000
2	1.036854	1.036862	1.024315	1.024402	1.024347	1.036920	1.036955	1.036935
3	1.036670	1.036686	1.024240	1.024414	1.024304	1.036803	1.036873	1.036832
4	1.036577	1.036587	1.024157	1.024352	1.024232	1.036719	1.036786	1.036741
5	1.035628	1.035613	1.023460	1.023938	1.023660	1.035944	1.036053	1.035936
6	1.026864	1.027041	1.018970	1.023079	1.020573	1.029849	1.031269	1.030329
7	1.018512	1.018936	1.014985	1.022727	1.017968	1.024186	1.027050	1.025331
8	1.016591	1.017081	1.014110	1.022715	1.017418	1.022905	1.026129	1.024231
9	1.015568	1.016082	1.013594	1.022625	1.017066	1.022197	1.025576	1.023580
10	1.006275	1.007258	1.009882	1.023342	1.015001	1.016355	1.021677	1.018765
11	1.004270	1.005312	1.008888	1.023192	1.014334	1.014995	1.020617	1.017509
12	1.000141	1.001599	1.008128	1.024915	1.014448	1.012878	1.019914	1.016405
13	0.994907	0.996663	1.006377	1.025848	1.013680	1.009764	1.018063	1.014021
14	0.990187	0.992279	1.005102	1.027164	1.013334	1.007112	1.016745	1.012228
15	0.986001	0.988472	1.004323	1.028877	1.013426	1.004940	1.015980	1.011046
16	0.985224	0.987767	1.004181	1.029198	1.013445	1.004538	1.015841	1.010830
17	0.983221	0.985768	1.003005	1.028746	1.012564	1.003082	1.014549	1.009327
18	0.983198	0.985745	1.002992	1.028741	1.012555	1.003066	1.014535	1.009311

Table A3. *Cont.*

Node	8:00	9:00	10:00	11:00	12:00	13:00	14:00	15:00
19	0.981957	0.984532	1.002386	1.028656	1.012150	1.002228	1.013874	1.008520
20	0.981159	0.983753	1.001996	1.028601	1.011890	1.001689	1.013449	1.008011
21	0.979870	0.982494	1.001370	1.028517	1.011474	1.000821	1.012766	1.007193
22	0.979844	0.982470	1.001366	1.028530	1.011476	1.000808	1.012763	1.007187
23	0.979788	0.982455	1.001523	1.028819	1.011671	1.000866	1.012943	1.007363
24	0.979665	0.982422	1.001866	1.029448	1.012096	1.000994	1.013337	1.007747
25	0.980074	0.983060	1.003163	1.031217	1.013498	1.001843	1.014809	1.009269
26	0.980243	0.983323	1.003698	1.031946	1.014076	1.002193	1.015416	1.009897
27	0.980526	0.983669	1.004152	1.032466	1.014532	1.002548	1.015929	1.010443
28	1.036619	1.036631	1.024195	1.024381	1.024266	1.036758	1.036824	1.036780
29	1.035984	1.035946	1.023633	1.023985	1.023789	1.036195	1.036226	1.036131
30	1.033768	1.033712	1.022275	1.023443	1.022766	1.034553	1.034714	1.034370
31	1.033377	1.033318	1.022035	1.023348	1.022586	1.034264	1.034447	1.034060
32	1.031421	1.031346	1.020837	1.022871	1.021684	1.032815	1.033113	1.032507
33	1.027880	1.027829	1.018919	1.022412	1.020342	1.030320	1.030988	1.029988
34	1.024897	1.025133	1.018588	1.024113	1.020712	1.028884	1.030658	1.029322
35	1.021550	1.021602	1.015779	1.022060	1.018281	1.026011	1.027515	1.025805
36	1.036565	1.036573	1.024145	1.024345	1.024223	1.036708	1.036775	1.036729
37	1.036276	1.036247	1.023864	1.024162	1.023995	1.036437	1.036499	1.036446
38	1.035987	1.035852	1.023561	1.024124	1.023836	1.036169	1.036243	1.036200
39	1.036046	1.035888	1.023599	1.024211	1.023902	1.036218	1.036305	1.036279
40	1.016704	1.017221	1.014310	1.022958	1.017624	1.023056	1.026358	1.024475
41	1.017399	1.018043	1.015311	1.024062	1.018616	1.023868	1.027489	1.025684
42	1.014464	1.015011	1.013125	1.022644	1.016773	1.021461	1.025043	1.022926
43	1.013331	1.013925	1.012709	1.022762	1.016544	1.020735	1.024567	1.022325
44	1.011876	1.012543	1.012239	1.023017	1.016325	1.019834	1.024025	1.021622
45	1.009856	1.010500	1.010969	1.022380	1.015307	1.018280	1.022572	1.019937
46	0.998978	0.999548	1.004321	1.019323	1.010096	1.010087	1.014980	1.011079
47	0.993617	0.994150	1.001045	1.017818	1.007528	1.006049	1.011239	1.006713
48	0.991539	0.992057	0.999776	1.017237	1.006534	1.004485	1.009790	1.005023
49	0.989552	0.990085	0.998718	1.016923	1.005762	1.003068	1.008564	1.003555
50	0.986812	0.987345	0.997202	1.016379	1.004615	1.001055	1.006789	1.001448
51	0.986365	0.986874	0.996830	1.016106	1.004293	1.000673	1.006374	1.000984
52	0.985857	0.986340	0.996407	1.015795	1.003926	1.000239	1.005903	1.000458
53	0.983370	0.983723	0.994336	1.014272	1.002127	0.998111	1.003594	0.997878
54	0.981728	0.981997	0.992961	1.013250	1.000928	0.996700	1.002067	0.996176
55	1.003817	1.004834	1.008511	1.022918	1.014009	1.014608	1.020196	1.017036
56	1.003812	1.004828	1.008507	1.022915	1.014005	1.014604	1.020191	1.017031
57	1.001369	1.003136	1.010108	1.027194	1.016449	1.014449	1.022176	1.018808
58	1.001380	1.003150	1.010123	1.027211	1.016464	1.014462	1.022194	1.018827
59	1.036616	1.036626	1.024191	1.024380	1.024263	1.036754	1.036821	1.036777
60	1.035968	1.035909	1.023601	1.023999	1.023783	1.036173	1.036212	1.036127
61	1.035542	1.035471	1.023375	1.024013	1.023658	1.035876	1.035995	1.035883
62	1.035419	1.035344	1.023310	1.024018	1.023621	1.035790	1.035932	1.035812
63	1.035411	1.035336	1.023304	1.024015	1.023617	1.035783	1.035926	1.035805
64	1.033154	1.032997	1.021852	1.023553	1.022591	1.034069	1.034434	1.034137
65	1.032331	1.032146	1.021351	1.023443	1.022255	1.033458	1.033930	1.033574
66	1.032222	1.032034	1.021285	1.023429	1.022211	1.033378	1.033863	1.033499
67	1.032198	1.032009	1.021269	1.023425	1.022201	1.033360	1.033848	1.033482
68	1.031909	1.031708	1.021087	1.023380	1.022078	1.033142	1.033665	1.033279
69	1.031908	1.031707	1.021087	1.023381	1.022078	1.033142	1.033665	1.033279
Node	**16:00**	**17:00**	**18:00**	**19:00**	**20:00**	**21:00**	**22:00**	**23:00**
1	1.050000	1.050000	1.050000	1.050000	1.050000	1.050000	1.050000	1.050000
2	1.036922	1.036901	1.036865	1.036860	1.036840	1.036869	1.024259	1.024297
3	1.036807	1.036765	1.036693	1.036684	1.036644	1.036702	1.024128	1.024204
4	1.036720	1.036671	1.036609	1.036606	1.036566	1.036630	1.024063	1.024148
5	1.035929	1.035808	1.035746	1.035777	1.035706	1.035861	1.023406	1.023609
6	1.029902	1.028795	1.027486	1.027374	1.026493	1.027860	1.016909	1.018692

Table A3. *Cont.*

Node	16:00	17:00	18:00	19:00	20:00	21:00	22:00	23:00
7	1.024376	1.022219	1.019494	1.019110	1.017344	1.019911	1.010451	1.013801
8	1.023135	1.020722	1.017639	1.017175	1.015190	1.018040	1.008931	1.012651
9	1.022436	1.019908	1.016676	1.016197	1.014117	1.017110	1.008178	1.012083
10	1.016754	1.012994	1.007666	1.006701	1.003433	1.007920	1.000850	1.006702
11	1.015389	1.011423	1.005789	1.004801	1.001348	1.006124	0.999413	1.005641
12	1.013520	1.008702	1.001431	0.999825	0.995489	1.001098	0.995422	1.002728
13	1.010554	1.004954	0.996334	0.994350	0.989237	0.995767	0.991236	0.999731
14	1.008103	1.001695	0.991620	0.989155	0.983224	0.990638	0.987205	0.996840
15	1.006186	0.998944	0.987304	0.984253	0.977461	0.985719	0.983336	0.994061
16	1.005832	0.998435	0.986503	0.983342	0.976390	0.984805	0.982617	0.993544
17	1.004324	0.996804	0.984747	0.981681	0.974638	0.983311	0.981442	0.992702
18	1.004307	0.996786	0.984727	0.981662	0.974617	0.983293	0.981428	0.992692
19	1.003462	0.995823	0.983595	0.980533	0.973384	0.982242	0.980605	0.992104
20	1.002919	0.995204	0.982867	0.979807	0.972591	0.981567	0.980076	0.991726
21	1.002044	0.994207	0.981691	0.978634	0.971308	0.980475	0.979219	0.991114
22	1.002033	0.994190	0.981664	0.978604	0.971272	0.980444	0.979196	0.991098
23	1.002129	0.994219	0.981545	0.978402	0.970994	0.980208	0.979014	0.990971
24	1.002339	0.994283	0.981287	0.977963	0.970387	0.979695	0.978617	0.990694
25	1.003420	0.995035	0.981258	0.977439	0.969467	0.978920	0.978022	0.990287
26	1.003865	0.995345	0.981246	0.977222	0.969088	0.978600	0.977777	0.990118
27	1.004289	0.995689	0.981386	0.977217	0.968981	0.978510	0.977708	0.990071
28	1.036758	1.036715	1.036650	1.036647	1.036609	1.036671	1.024102	1.024183
29	1.036156	1.036094	1.036127	1.036195	1.036179	1.036288	1.023779	1.023924
30	1.034432	1.034262	1.034231	1.034454	1.034374	1.034757	1.022597	1.023108
31	1.034128	1.033939	1.033896	1.034146	1.034056	1.034487	1.022388	1.022964
32	1.032607	1.032323	1.032223	1.032610	1.032464	1.033137	1.021345	1.022245
33	1.030036	1.029493	1.029097	1.029615	1.029274	1.030425	1.019243	1.020784
34	1.028795	1.027611	1.026027	1.026116	1.025144	1.026921	1.016536	1.018914
35	1.025646	1.024551	1.023424	1.024068	1.023278	1.025335	1.015306	1.018058
36	1.036709	1.036658	1.036599	1.036595	1.036556	1.036620	1.024055	1.024140
37	1.036429	1.036340	1.036338	1.036341	1.036301	1.036383	1.023839	1.023948
38	1.036159	1.035928	1.036075	1.036046	1.035987	1.036104	1.023601	1.023756
39	1.036217	1.035942	1.036114	1.036058	1.035987	1.036104	1.023601	1.023756
40	1.023319	1.020863	1.017686	1.017152	1.015119	1.017978	1.008880	1.012611
41	1.024276	1.021661	1.018077	1.017245	1.015018	1.017892	1.008812	1.012562
42	1.021738	1.019063	1.015635	1.015133	1.012937	1.016094	1.007368	1.011489
43	1.021070	1.018220	1.014540	1.013987	1.011646	1.014983	1.006479	1.010834
44	1.020259	1.017162	1.013115	1.012472	1.009922	1.013500	1.005299	1.009968
45	1.018674	1.015470	1.011376	1.010891	1.008291	1.012100	1.004186	1.009157
46	1.010247	1.006497	1.002052	1.002408	0.999517	1.004627	0.998342	1.005010
47	1.006094	1.002075	0.997457	0.998228	0.995193	1.000944	0.995462	1.002966
48	1.004484	1.000362	0.995676	0.996607	0.993517	0.999516	0.994346	1.002176
49	1.003053	0.998788	0.993939	0.994978	0.991787	0.998053	0.993219	1.001397
50	1.001047	0.996571	0.991538	0.992740	0.989420	0.996038	0.991644	1.000281
51	1.000630	0.996164	0.991187	0.992460	0.989163	0.995818	0.991470	1.000155
52	1.000156	0.995701	0.990789	0.992142	0.988870	0.995567	0.991271	1.000010
53	0.997834	0.993433	0.988836	0.990582	0.987436	0.994336	0.990295	0.999300
54	0.996298	0.991932	0.987537	0.989536	0.986470	0.993502	0.989624	0.998800
55	1.014965	1.011010	1.005436	1.004523	1.001094	1.005909	0.999246	1.005525
56	1.014960	1.011005	1.005432	1.004520	1.001091	1.005906	0.999244	1.005524
57	1.015372	1.010197	1.001976	0.999742	0.994961	1.000641	0.995052	1.002452
58	1.015387	1.010209	1.001982	0.999743	0.994960	1.000639	0.995051	1.002451
59	1.036755	1.036710	1.036647	1.036643	1.036605	1.036666	1.024098	1.024180
60	1.036139	1.036042	1.036101	1.036150	1.036125	1.036237	1.023730	1.023878
61	1.035851	1.035666	1.035688	1.035706	1.035633	1.035805	1.023374	1.023605
62	1.035768	1.035558	1.035569	1.035578	1.035490	1.035680	1.023272	1.023526
63	1.035761	1.035551	1.035562	1.035571	1.035483	1.035674	1.023267	1.023522

Table A3. *Cont.*

Node	16:00	17:00	18:00	19:00	20:00	21:00	22:00	23:00
64	1.034021	1.033528	1.033507	1.033525	1.033307	1.033767	1.021700	1.022318
65	1.033411	1.032793	1.032740	1.032739	1.032457	1.033021	1.021083	1.021840
66	1.033330	1.032696	1.032639	1.032635	1.032345	1.032922	1.021002	1.021777
67	1.033312	1.032674	1.032616	1.032612	1.032320	1.032901	1.020984	1.021763
68	1.033093	1.032411	1.032349	1.032339	1.032027	1.032643	1.020770	1.021597
69	1.033093	1.032411	1.032348	1.032338	1.032026	1.032642	1.020769	1.021596

References

1. Cossent, R.; Gómez, T.; Olmos, L.; Gómez, T. Large-scale integration of renewable and distributed generation of electricity in Spain: Current situation and future needs. *Energy Policy* **2011**, *39*, 8078–8087. [CrossRef]
2. Schonardie, M.F.; Martins, D.C. Application of the dq0 transformation in the three-phase grid-connected PV systems with active and reactive power control. In Proceedings of the 2008 IEEE International Conference on Sustainable Energy Technologies, Singapore, 24–27 November 2008; pp. 18–23.
3. *Reference Technical Rules for the Connection of Active and Passive Consumers to the HV and MV Electrical Networks of Distribution Company Issue*; Italian Technical Guidelines CEI 0-16 2012-12; Comitato Elettrotecnico Italiano: Milan, Italy, 2012.
4. Thomson, M.; Infield, D. Impact of widespread photovoltaics generation on distribution systems. *IET Renew. Power Gener.* **2007**, *1*, 33. [CrossRef]
5. Tonkoski, R.; Lopes, L.A.C.; El-Fouly, T.H.M. Coordinated Active Power Curtailment of Grid Connected PV Inverters for Overvoltage Prevention. *IEEE Trans. Sustain. Energy* **2010**, *2*, 139–147. [CrossRef]
6. Zhao, C.; Gu, C.; Li, F.; Dale, M. Understanding LV network voltage distribution- UK smart grid demonstration experience. In Proceedings of the 2015 IEEE Power & Energy Society Innovative Smart Grid Technologies Conference (ISGT), Washington, DC, USA, 18–20 February 2015; pp. 1–5.
7. Dou, X.; Duan, X.; Hu, Q.; Shen, L.; Wu, Z. A nonintrusive control strategy using voltage and reactive power for distribution systems based on PV and the nine-zone diagram. *Int. J. Electr. Power Energy Syst.* **2019**, *105*, 89–97. [CrossRef]
8. Zhu, Y.; Tomsovic, K. Adaptive power flow method for distribution systems with dispersed generation. *IEEE Trans. Power Deliv.* **2002**, *17*, 822–827. [CrossRef]
9. Valverde, G.; Van Cutsem, T.H. Model Predictive Control of Voltages in Active Distribution Networks. *IEEE Trans. Smart Grid* **2013**, *4*, 2152–2161. [CrossRef]
10. Robbins, B.A.; Hadjicostis, C.N.; Domínguez-García, A.D. A Two-Stage Distributed Architecture for Voltage Control in Power Distribution Systems. *IEEE Trans. Power Syst.* **2012**, *28*, 1470–1482. [CrossRef]
11. Sulc, P.; Backhaus, S.; Chertkov, M. Optimal Distributed Control of Reactive Power via the Alternating Direction Method of Multipliers. *IEEE Trans. Energy Convers.* **2014**, *29*, 968–977. [CrossRef]
12. Calderaro, V.; Galdi, V.; Massa, G.; Piccolo, A. Distributed generation management: An optimal sensitivity approach for decentralized power control. In Proceedings of the 2012 3rd IEEE PES Innovative Smart Grid Technologies Europe (ISGT Europe), Berlin, Germany, 14–17 October 2012; pp. 1–8. [CrossRef]
13. Calderaro, V.; Conio, G.; Galdi, V.; Massa, G.; Piccolo, A. Optimal Decentralized Voltage Control for Distribution Systems with Inverter-Based Distributed Generators. *IEEE Trans. Power Syst.* **2013**, *29*, 230–241. [CrossRef]
14. Turitsyn, K.; Sulc, P.; Backhaus, S.; Chertkov, M. Options for Control of Reactive Power by Distributed Photovoltaic Generators. *Proc. IEEE* **2011**, *99*, 1063–1073. [CrossRef]
15. Cai, Y.; Tang, W.; Li, L.; Zhang, B.; Zhang, L.; Wang, Y. Multi-mode adaptive local reactive power control method based on PV inverters in low voltage distribution networks. *IET Gener. Transm. Distrib.* **2020**, *14*, 542–551. [CrossRef]
16. Molina-Garcia, A.; Mastromauro, R.A.; Garcia-Sanchez, T.; Pugliese, S.; Liserre, M.; Stasi, S. Reactive Power Flow Control for PV Inverters Voltage Support in LV Distribution Networks. *IEEE Trans. Smart Grid* **2016**, *8*, 447–456. [CrossRef]

17. Dickert, J.; Domagk, M.; Schegner, P. Benchmark low voltage distribution networks based on cluster analysis of actual grid properties. In Proceedings of the 2013 IEEE Grenoble Conference, Grenoble, France, 16–20 June 2013; pp. 1–6.
18. Kabir, M.N.; Mishra, Y.; Ledwich, G.; Dong, Z.Y.; Wong, K.P. Coordinated Control of Grid-Connected Photovoltaic Reactive Power and Battery Energy Storage Systems to Improve the Voltage Profile of a Residential Distribution Feeder. *IEEE Trans. Ind. Inform.* **2014**, *10*, 967–977. [CrossRef]
19. Mumtaz, F.; Syed, M.H.; Al Hosani, M.; Zeineldin, H.H. A Novel Approach to Solve Power Flow for Islanded Microgrids Using Modified Newton Raphson with Droop Control of DG. *IEEE Trans. Sustain. Energy* **2015**, *7*, 493–503. [CrossRef]
20. Biserica, M.; Berseneff, B.; Besanger, Y.; Kieny, C. Upgraded Coordinated Voltage Control for Distribution Systems. In Proceedings of the IEEE Trondheim PowerTech, Trondheim, Norway, 19–23 June 2011; pp. 1–6. [CrossRef]
21. Zhang, B.; Lam, A.Y.S.; Dominguez-Garcia, A.D.; Tse, D. An Optimal and Distributed Method for Voltage Regulation in Power Distribution Systems. *IEEE Trans. Power Syst.* **2014**, *30*, 1714–1726. [CrossRef]
22. Ahmed, M.; Bhattarai, R.; Hossain, S.J.; Abdelrazek, S.; Kamalasadan, S. Coordinated voltage control strategy for voltage regulators and voltage source converters integrated distribution system. In Proceedings of the 2017 IEEE Industry Applications Society Annual Meeting, Harbor, MD, USA, 14–17 January 2017; pp. 1–8.
23. Castillo, A.; Gayme, D.F. Profit maximizing storage allocation in power grids. In Proceedings of the 52nd IEEE Conference on Decision and Control, Florence, Italy, 10–13 December 2013; pp. 429–435.
24. Bose, S.; Gayme, D.F.; Topcu, U.; Chandy, K.M.; Bose, S. Optimal placement of energy storage in the grid. In Proceedings of the 2012 IEEE 51st IEEE Conference on Decision and Control (CDC), Maui, HI, USA, 10–13 December 2012; pp. 5605–5612.
25. Nasrolahpour, E.; Kazempour, S.; Zareipour, H.; Rosehart, W.D. Strategic Sizing of Energy Storage Facilities in Electricity Markets. *IEEE Trans. Sustain. Energy* **2016**, *7*, 1462–1472. [CrossRef]
26. Nick, M.; Cherkaoui, R.; Paolone, M. Optimal siting and sizing of distributed energy storage systems via alternating direction method of multipliers. *Int. J. Electr. Power Energy Syst.* **2015**, *72*, 33–39. [CrossRef]
27. Yan, W.; Yu, J.; Yu, D.; Bhattarai, K. A new optimal reactive power flow model in rectangular form and its solution by predictor corrector primal dual interior point method. *IEEE Trans. Power Syst.* **2006**, *21*, 61–67. [CrossRef]
28. Esmin, A.; Lambert-Torres, G.; De Souza, A.Z. A hybrid particle swarm optimization applied to loss power minimization. *IEEE Trans. Power Syst.* **2005**, *20*, 859–866. [CrossRef]
29. Li, Y.; Li, M.; Wu, Q. Optimal reactive power dispatch with wind power integrated using group search optimizer with intraspecific competition and lévy walk. *J. Mod. Power Syst. Clean Energy* **2014**, *2*, 308–318. [CrossRef]
30. Farivar, M.; Low, S.H. Branch Flow Model: Relaxations and Convexification—Part I. *IEEE Trans. Power Syst.* **2013**, *28*, 2554–2564. [CrossRef]
31. Wang, C.; Xiang, L.; Deng, Z.; Liang, Z. Reactive Power Optimization Dispatch Strategy in Distribution Network with Distributed Generators. *J. Eng.* **2017**, *2017*, 1418–1422. [CrossRef]
32. Chen, L.; Deng, Z.; Xu, X. Two-Stage Dynamic Reactive Power Dispatch Strategy in Distribution Network Considering the Reactive Power Regulation of Distributed Generations. *IEEE Trans. Power Syst.* **2018**, *34*, 1021–1032. [CrossRef]
33. Maciejowski, J.M. *Predictive Control with Constraints*; Prentice-Hall: Englewood Cliffs, NJ, USA, 2002.
34. Glavic, M.; Hajian, M.; Rosehart, W.; Van Cutsem, T.H. Receding-Horizon Multi-Step Optimization to Correct Nonviable or Unstable Transmission Voltages. *IEEE Trans. Power Syst.* **2011**, *26*, 1641–1650. [CrossRef]
35. Fortenbacher, P.; Ulbig, A.; Andersson, G. Optimal Placement and Sizing of Distributed Battery Storage in Low Voltage Grids Using Receding Horizon Control Strategies. *IEEE Trans. Power Syst.* **2017**, *33*, 2383–2394. [CrossRef]
36. Hug-Glanzmann, G. Coordination of intermittent generation with storage, demand control and conventional energy sources. In Proceedings of the 2010 IREP Symposium Bulk Power System Dynamics and Control—VIII (IREP), Rio de Janeiro, Brazil, 1–6 August 2010; pp. 1–7. [CrossRef]
37. Bolognani, S.; Zampieri, S. On the Existence and Linear Approximation of the Power Flow Solution in Power Distribution Networks. *IEEE Trans. Power Syst.* **2015**, *31*, 163–172. [CrossRef]

38. Yang, Z.; Wu, R.; Yang, J.; Long, K.; You, P. Economical Operation of Microgrid with Various Devices Via Distributed Optimization. *IEEE Trans. Smart Grid* **2015**, *7*, 1–11. [CrossRef]
39. Nick, M.; Cherkaoui, R.; Paolone, M. Optimal Allocation of Dispersed Energy Storage Systems in Active Distribution Networks for Energy Balance and Grid Support. *IEEE Trans. Power Syst.* **2014**, *29*, 2300–2310. [CrossRef]
40. Niknam, T.; Zare, M.; Aghaei, J. Scenario-Based Multiobjective Volt/Var Control in Distribution Networks Including Renewable Energy Sources. *IEEE Trans. Power Deliv.* **2012**, *27*, 2004–2019. [CrossRef]
41. Baran, M.; Wu, F. Optimal capacitor placement on radial distribution systems. *IEEE Trans. Power Deliv.* **1989**, *4*, 725–734. [CrossRef]
42. GUROBI. Available online: http://www.gurobi.com (accessed on 22 February 2018).
43. National Bureau of Quality Supervision. *Inspection and Quarantine and National Standardization Management Committee. National Standard of the People's Republic of China GB/T12325-2008 Power Quality and Voltage Deviation*; National Bureau of Quality Supervision: Beijing, China, 2008.
44. Zhang, Y.-J.; Ren, Z. Optimal Reactive Power Dispatch Considering Costs of Adjusting the Control Devices. *IEEE Trans. Power Syst.* **2005**, *20*, 1349–1356. [CrossRef]
45. Wong, T. Co-ordination of transformer tap and capacitor operation for reactive power voltage control in a distribution primary substation. In Proceedings of the APSCOM 2000—5th International Conference on Advances in Power System Control, Operation and Management, Hong Kong, China, 30 October–1 November 2000; Volume 2000, pp. 479–485.
46. Sun, C.; Xu, J.; Cai, B.; Yang, Z.; Li, X. Research on efficiency increase of the automatic voltage control system in Shanghai urban power grid. In Proceedings of the 8th Renewable Power Generation Conference (RPG 2019), Shanghai, China, 24–25 October 2019; pp. 1–6.
47. Khan, I.; Li, Z.; Xu, Y.; Gu, W. Distributed control algorithm for optimal reactive power control in power grids. *Int. J. Electr. Power Energy Syst.* **2016**, *83*, 505–513. [CrossRef]